

**Aus dem Zentrum für Neurologie der Universität Tübingen  
Abteilung Kognitive Neurologie  
Ärztlicher Direktor: Professor Dr. H. P. Thier  
Sektion Neuropsychologie  
Leiter: Professor Dr. Dr. H.-O. Karnath  
und  
dem Max-Planck Institut für Biologische Kybernetik Tübingen  
Abteilung Cognitive and Computational Psychophysics  
Direktor: Professor Dr. H. H. Bülthoff**

**Temporal and spatial properties of shape processing  
in the human visual cortex:  
Combined fMRI and MEG adaptation**

**Inaugural-Dissertation  
zur Erlangung des Doktorgrades der Medizin  
der Medizinischen Fakultät  
der Eberhard Karls Universität zu Tübingen**

**vorgelegt  
von Elisabeth Huberle  
aus Berlin**

2006

Dekan: Professor Dr. I. B. Autenrieth

1. Berichterstatter: Professor Dr. Dr. H.-O. Karnath

2. Berichterstatter: Professor Dr. W. Grodd



# Statement

Ich erkläre hiermit, dass ich die der Medizinischen Fakultät der Universität Tübingen zur Promotion eingereichte Arbeit mit dem Titel: "Temporal and spatial properties of shape processing in the human visual cortex: Combined fMRI and MEG adaptation" selbständig ohne unzulässige Hilfe Dritter und ohne Benutzung anderer als der angegebenen Hilfsmittel angefertigt habe; die aus fremden Quellen direkt oder indirekt übernommenen Gedanken sind als solche kenntlich gemacht. Ich versichere an Eides statt, dass diese Angaben wahr sind und dass ich nichts verschwiegen habe. Mir ist bekannt, dass die falsche Abgabe einer Versicherung an Eides statt mit einer Freiheitsstrafe bis zu drei Jahren oder mit einer Geldstrafe bestraft wird.

[Elisabeth Huberle]



# Contents

<b>1</b>	<b>Introduction</b>	<b>1</b>
1.1	Visual system . . . . .	1
1.1.1	From the retina to primary visual cortex . . . . .	1
1.1.2	Primary visual cortex . . . . .	2
1.1.3	Visual pathways . . . . .	3
1.1.4	Higher object-related visual areas . . . . .	4
1.2	Shape processing in the visual system . . . . .	4
1.2.1	Spatial properties of shape processing . . . . .	4
1.2.2	Temporal properties of shape processing . . . . .	5
1.3	Neurophysiological approaches . . . . .	6
1.3.1	Principles of functional magnetic resonance imaging . . . . .	6
1.3.2	Spatial encoding in fMRI . . . . .	7
1.3.3	Blood oxygenation level dependent and temporal encoding in fMRI . . . . .	8
1.3.4	fMRI adaptation and neuronal adaptation . . . . .	9
1.3.5	Principles of magnetoencephalography . . . . .	12
1.3.6	Spatial encoding in MEG . . . . .	12
1.3.7	Combined fMRI and MEG investigation . . . . .	14
1.4	Purpose of investigation . . . . .	15

<b>2</b>	<b>Methods and Material</b>	<b>17</b>
2.1	Observers . . . . .	17
2.2	Visual stimuli . . . . .	17
2.2.1	Visual stimuli for Experiments 1 to 3 . . . . .	17
2.2.2	Visual stimuli for Experiment 4 . . . . .	19
2.2.3	Visual stimuli for Experiment 5 . . . . .	20
2.2.4	Visual stimuli for LOC localizer . . . . .	20
2.2.5	Visual stimuli for localizers of retinotopic areas . . . . .	22
2.3	Design and task . . . . .	23
2.3.1	General structure . . . . .	23
2.3.2	Design and task for Experiment 1 and 2 . . . . .	23
2.3.3	Design and task for Experiment 3 . . . . .	24
2.3.4	Design and task for Experiment 4 . . . . .	25
2.3.5	Design and task for Experiment 5 . . . . .	25
2.3.6	Design and task for localizer scans . . . . .	26
2.4	Data acquisition . . . . .	26
2.5	Data analysis . . . . .	27
2.5.1	General structure for fMRI data . . . . .	27
2.5.2	Regions of interest . . . . .	27
2.5.3	Timecourse analysis of fMRI data . . . . .	30
2.5.4	General structure for MEG data . . . . .	34
2.5.5	Field of Interest . . . . .	34
2.5.6	Timecourse analysis of MEG data . . . . .	35
2.6	Psychophysical Data . . . . .	37
2.6.1	General structure . . . . .	37

2.6.2	Psychophysical Data for Experiment 1 and 3 . . . . .	37
2.6.3	Psychophysical Data for Experiment 4 . . . . .	38
2.7	Eye-movement data . . . . .	39
2.7.1	Eye-movement data for Experiment 1 . . . . .	39
2.7.2	Eye-movement data for Experiment 2 . . . . .	40
2.7.3	Comparison of eye-movement data for Experiment 1 & 2 . . . . .	41
2.7.4	Eye-movements for Experiment 4 . . . . .	42
2.7.5	Eye-movements for Experiment 5 . . . . .	43
<b>3</b>	<b>Results</b>	<b>45</b>
3.1	Results for Experiment 1 . . . . .	45
3.2	Results for Experiment 2 . . . . .	48
3.3	Results for Experiment 3 . . . . .	50
3.4	Results for Experiment 4 . . . . .	51
3.5	Results for Experiment 5 . . . . .	54
<b>4</b>	<b>Discussion</b>	<b>57</b>
4.1	Combined fMRI and MEG studies . . . . .	57
4.2	Temporal characteristics . . . . .	58
4.3	Spatial characteristics . . . . .	60
4.4	Attention and shape processing . . . . .	62
4.5	Outlook . . . . .	63
<b>5</b>	<b>Conclusions</b>	<b>65</b>
<b>6</b>	<b>Summary</b>	<b>67</b>
<b>7</b>	<b>References</b>	<b>69</b>

<b>8 Appendix</b>	<b>81</b>
8.1 Abbreviations . . . . .	81
8.2 Supplementary figures . . . . .	83
<b>9 Acknowledgements</b>	<b>85</b>
<b>10 Curriculum vitae</b>	<b>87</b>

# Chapter 1

## Introduction

### 1.1 Visual system

#### 1.1.1 From the retina to primary visual cortex

The visual system is one of the most complex systems and a large number of neurons in the primate brain are involved in the processing of visual information. Based on neurophysiological studies, the percentage of cortical neurons involved in visual analysis is higher than fifty percent in the monkey brain (De Yoe & Van Essen, 1988). Amongst the most prominent processing relays in the primate brain are the eyes with the retina, optic nerves, lateral geniculate nucleus, as well as primary and secondary visual cortex.

After the first steps of visual processing in the retina, visual information is transmitted to the optic chiasma via the optic nerves, where nasal axons cross to the opposite side while temporal axons remain on their original side. That is, visual information of the right visual hemifield is further transmitted to the left hemisphere of the brain and vice versa. Through the optic tracts, the visual input is then sent to the lateral geniculate nucleus (LGN) of the thalamus, from where information is relayed via the optic radiation to the primary visual cortex .

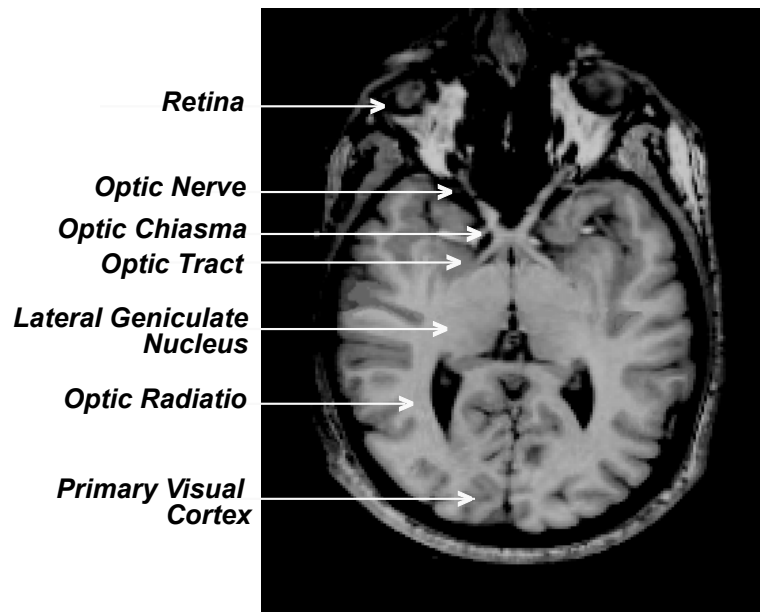


Figure 1.1: The major components of the visual system displayed on an anatomical MRI scan of a representative human observer

### 1.1.2 Primary visual cortex

Primary visual cortex - also known as striate cortex, Brodman Area 17 or V1 - is located around the calcarine fissure in the occipital lobe (see also Figure 2.7) and shows a retinotopic organization (Tiao & Blakemore, 1978). That is, adjacent locations of the visual field are represented at adjacent locations in the cortex with the center of the visual field being represented at the occipital pole. Central retinal areas, which fall near to or onto the fovea, receive proportionally greater representation in primary visual cortex than peripheral areas (Cortical Magnification Factor) (Tiao & Blakemore, 1978; Tootell et al., 1988). Functionally, neurons within primary visual cortex are involved in the analysis of local level image features: neurons function as edge or line detectors and show strong responses for a preferred orientation as well as contrast sensitivity (Essen & Zeki, 1978; Foster et al., 1985). These early stages of visual processing mediate the detection of lines and edges in an image. Due to the small size of receptive fields (area which is being processed by an individual neuron) in primary visual cortex (around  $0.5^\circ$  at central positions and around  $1.0^\circ$  at peripheral location), objects may not be processed as a whole.

### 1.1.3 Visual pathways

From V1, visual information is then forwarded to a series of centers located in the posterior temporal and parietal lobe. Ungerleider and Mishkin (1982) proposed different neural pathways for the processing of visual information about properties such as color, shape, depth and motion: Cortical centers in the temporal lobe along the so-called "ventral pathway" (also known as "What ?" - System) are involved in object recognition, whereas parietal and medial temporal centers of the "dorsal pathway" (or "Where?" - System) analyze the location and motion of objects. However, alternative approaches (Milner & Goodale, 1995) suggested that the dorsal pathway is also involved in spatially guided motor behavior such as reaching and formed the term "How ?" - System.

In the visual cortex, over thirty different visual areas along the ventral and dorsal pathway have been identified (De Yoe & Van Essen, 1988). Specifically, areas involved at rather early stages of cortical processing along the ventral pathway are areas V2, VP and V4; in parallel to V1, these areas show a retinotopic organization, have small receptive field sizes and are involved in the analysis of local information of objects (Grill-Spector, 1998b). Furthermore, these areas are considered as the early visual areas (including V1). Following the ventral pathway, adjacent to V4, the Lateral Occipital Complex (LOC) is situated.

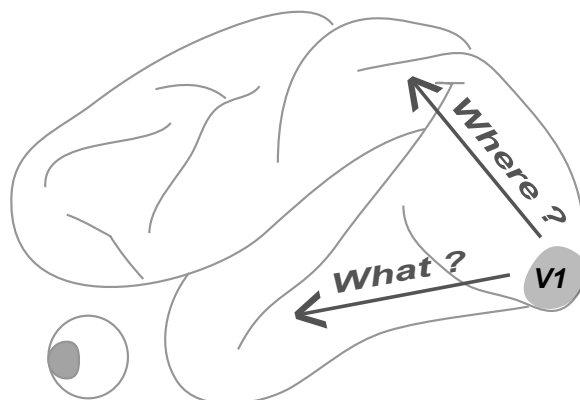


Figure 1.2: Schematic display of the ventral ("What ?" - System) and dorsal ("Where ?" - System) visual pathway in the human brain.

### **1.1.4 Higher object-related visual areas**

The LOC is located lateral in the occipital lobe and extends anterior in the posterior fusiform gyrus (see also Figure 2.7 and 2.8). It has been suggested to be involved in the analysis of shape information and plays a critical role in object recognition (Malach et al., 1995). Responses are selective to objects independent of their size and position (Grill-Spector et al., 1998a, 1999). Functionally, the LOC has been proposed to be a homologue of the monkey IT (Denys et al., 2004). Two separate subdivisions of the LOC were identified previously (e.g. Grill-Spector et al., 1999): the more posterior located lateral occipital region (LO) and in relation anterior located regions in the posterior fusiform gyrus (pFs). Kourtzi and Kanwisher (2001) suggested, that the LOC represents the global perceived shape of objects rather than their low level features. Further studies proposed a correlation between the global percept of shapes and the activation of neural populations in the LOC (Grill-Spector et al., 2000).

## **1.2 Shape processing in the visual system**

### **1.2.1 Spatial properties of shape processing**

The recognition of objects in our complex environments requires the extraction of information about their properties and the interpretation of the shape structure. The investigation of shape processing in the human and monkey visual system as well as the characterization of shape representation have been the central goal for theoretical (Riesenhuber & Poggio, 1999, 2000), neurophysiological (Logothetis & Sheinberg, 1996) and imaging (Grill-Spector, 2003) approaches. However, at the current stage of investigation, many questions about the integration of local elements into global shapes remain open. In detail, the question at what stage of cortical processing is global shape analysis performed is unclear. Recent fMRI studies (Lerner et al., 2001) proposed a hierarchical axis of shape processing in the human visual cortex, that extends from the early to higher visual areas



of the ventral visual pathway. In accordance, previous work (Maunsell & Newsome, 1987; Felleman & Van Essen, 1991; Van Essen et al., 1992) suggested the involvement of early visual areas in the analysis of local image features, while higher visual areas of the ventral visual pathway mediate the perception and recognition of global shapes. In contrast, alternative approaches (Allman et al., 1985; Gilbert, 1992, 1998; Lamme et al., 1998; Altmann et al., 2003; Kourtzi et al., 2003b) provided evidence for an involvement of the early visual areas in the processing of shape information at a global scale: The integration of local features into global shapes in these areas extended the size of classical receptive fields and suggested therefore a role of early visual areas in integration processes in a rather global manner.

### **1.2.2 Temporal properties of shape processing**

What is the timecourse of shape processing across early and higher visual areas? Traditionally, a feedforward model of shape processing has been suggested, in which visual information is transmitted from the retina via primary visual cortex to higher visual areas (Fukushima, 1980; Riesenhuber & Poggio, 1999; Van Rullen & Thorpe, 2001). Hereby, responses in V1 start as early as 20 msec after stimulus presentation, peak at 50-60 msec and disappear the latest at 90-120 msec (for review see Bullier, 2001). Further, it has been shown, that the earliest response latencies in the occipitotemporal areas arise 100 msec after stimulus presentation, peak at 130 msec and disappear at 200 msec (Goebel et al., 1998). Following this model, integration processes extend from early to higher visual areas. In contrast, other investigators proposed the involvement of cortico-cortical feedback connections from higher to early visual areas in the processing of shape information (Edelman, 1992; Nowak & Bullier, 1998; Roelfsema et al., 1998, Lamme & Roelfsema, 2000). These feedback connections might play a critical role, when the stimulus reaches a perceptual level (Super et al., 2001) and are likely required for conscious visual perception (Bullier et al., 2001). Further theories on predictive coding (Rao & Ballard, 1999; Murray et al., 2002, 2004) suggested that the processing at early stages of visual analysis reflects the residual error after com-

parison of the physical input to the perceptual interpretation computed in higher areas. Therefore, the proposed involvement of feedback mechanisms indicated a rather late involvement of early visual areas in integration processes.

## 1.3 Neurophysiological approaches

### 1.3.1 Principles of functional magnetic resonance imaging

Over the past decade, functional magnetic resonance imaging (fMRI) has become a well-established non-invasive tool to investigate the functional properties of the primate brain. The theoretical background of fMRI is based on Magnetic Resonance Imaging (MRI) methods that have been developed by Felix Bloch and Edward Purcell in the middle of the twentieth century.

The primate body mainly consists of water, of which the protons partly align during the presence of a strong magnetic field  $B_0$  ( $> 1$  Tesla) in parallel or anti-parallel. This alignment results in a longitudinal net magnetization. Applying a radiofrequency (RF) pulse ( $B_1$ -field), that follows the Larmor equation ( $f = \gamma * B_0$ ,  $\gamma_{protons} = 42.58 \text{ MHz/T}$ ), for approximately three to four milliseconds perpendicular to the  $B_0$ -field induces a misalignment of protons resulting therefore in a transverse magnetization. The Time to Echo (TE) describes the time between the application of the RF-pulse and data acquisition, whereas the temporal interval between two RF-pulses at identical positions has been termed the Time to Repetition (TR).

T1-weighted images are sensitive to the recovery of the longitudinal magnetization and T2-weighted images to changes in the transverse magnetization after a RF pulse.

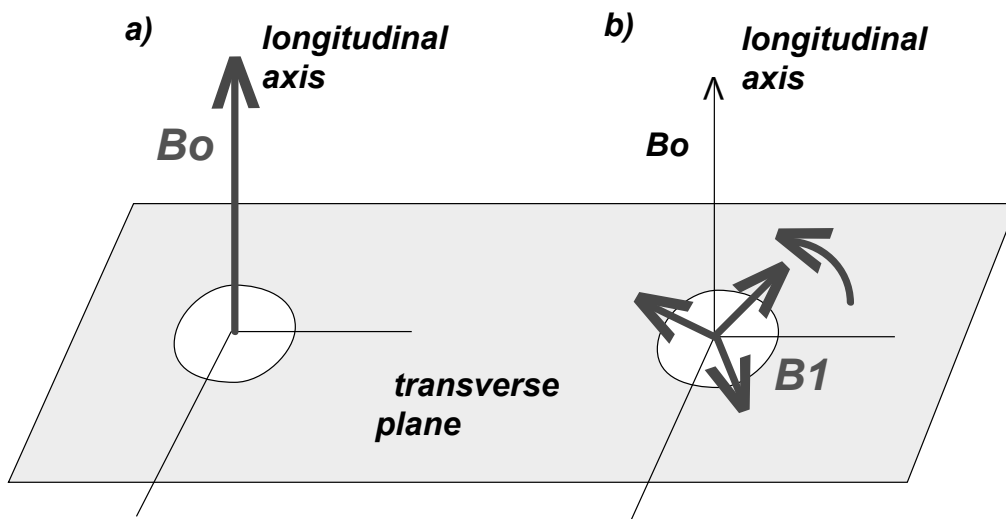


Figure 1.3: Principles of MRI. a) Protons align with a magnetic field  $B_0$  resulting in a longitudinal net magnetization. b) A misalignment of these protons is achieved by applying a radiofrequency pulse ( $B_1$ -field) perpendicular to the  $B_0$ -field resulting in a transverse magnetization.

### 1.3.2 Spatial encoding in fMRI

MRI and fMRI use the same principals for the encoding of spatial position in a three-dimensional array. The size of a volumetric pixel - the so-called "voxel" - determines the resolution of this array. The resolution of the array used in the present experiments was  $256 \times 256 \times 11$  resulting in a voxel size of  $3\text{mm} \times 3\text{mm} \times 5\text{mm}$ . In this array, the x-coordinate is determined by the frequency of the RF-pulse that results from an additional weak gradient added to the  $B_0$ -field (see Larmor equation), the y-coordinate by the phase and the z-coordinate by the slice.

### 1.3.3 Blood oxygenation level dependent and temporal encoding in fMRI

fMRI is sensitive to changes in the blood oxygenation level dependent (BOLD) effect in sequences termed  $T2^*$ , that was first discovered by Ogawa and colleagues (1990a, 1990b). To a large degree, the BOLD effect reflects the relation between oxy- and desoxyhemoglobin: Neuronal activity requires energy consumption and results in both increased cerebral blood flow (CBF) and cerebral blood volume (CBV). After a short initial decrease of blood oxygenation, the blood oxygenation exceeds its original level due to increased CBF and CBV. That is, the relation between oxy- and desoxyhemoglobin increases with neuronal activity. As a consequence of the different magnetic properties of oxy- and desoxyhemoglobin - desoxyhemoglobin is paramagnetic and introduces an inhomogeneity into nearby magnetic field, whereas oxyhemoglobin is weakly diamagnetic and has little effect - this elevated relation between oxy- and desoxyhemoglobin can be detected. Recent studies by Logothetis and colleagues (2001) provided strong evidence for a high correlation between the BOLD effect and local field potentials, which are believed to reflect the spiking activity of neurons (for review see Heeger & Ress, 2002), and thus strengthened the role of fMRI as a sensitive non-invasive tool to investigate cortical functions in the primate brain.

The hemodynamic response function (HRF) reflects the timecourse of the BOLD signal. After an initial dip of the hemodynamic response function the signal peaks three to five seconds after stimulus presentation, followed by a short undershoot, and returns to baseline at a latency of eight to ten seconds. However, the prolonged timecourse of the hemodynamic response function restricts the temporal resolution of fMRI to the range of seconds.

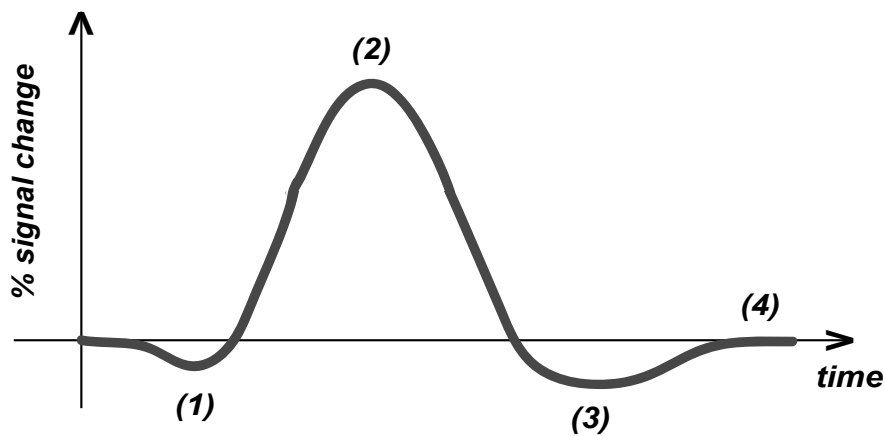


Figure 1.4: Schematic display of the timecourse of the hemodynamic response function (HRF): an initial dip (1) is observed before the HRF peaks (2) between three and five seconds after the stimulus presentation (SP), followed by a short undershoot (3). Finally, the HRF returns to baseline (4) eight to ten seconds after SP.

### 1.3.4 fMRI adaptation and neuronal adaptation

fMRI adaptation has been established as a tool to overcome the limited spatial resolution of conventional fMRI, that averages across neuronal populations represented in one voxel which may respond differentially to different stimulus attributes (Raymond et al., 1998; Grill-Spector et al., 1999; Grill-Spector et al., 2001; Kourtzi et al., 2003a). fMRI adaptation focuses on decreased responses for repeated stimulus presentation. That is, the BOLD signal for consecutively identical stimuli is expected to be lower than for stimuli with different properties. By comparing the adapted response evoked by the same stimuli with the increased responses evoked by different stimuli, sensitivity in the neural populations to changes in the stimulus properties can be deduced. fMRI adaptation has been shown to not only occur in occipital (Grill-Spector et al., 1999; Kourtzi & Kanwisher, 2000), but also parietal and frontal areas (Naccache & Dehaene, 2001) and has been used extensively to study functional properties of the primate brain (Tootell et al., 1995,

1998; Buckner et al., 1998a, 1998b; Grill-Spector et al., 1999; Engel & Furmanski, 2001; Huk et al., 2001; Naccache & Dehaene, 2001; Avidan et al., 2002; Vuilleumier et al., 2002).

What is the benefit of adaptation? The advantage of neuronal adaptation can be found in reduced energy consumption. fMRI adaptation follows neuronal adaptation (Carandini et al., 1997; Lisberger and Movshon, 1999; Müller et al., 1999) and repetition suppression effects (Miller et al., 1991; Li et al., 1993; Desimone, 1996), whereby neural activity is decreased for repeated stimuli. The "neuronal sharpening theory" by Wiggs and Martin (1998) predicted, that neurons insensitive to certain stimulus properties decrease their firing rates, whereas those neurons that play a critical role in the processing of distinct stimulus properties show robust responses. Alternative approaches can be found in shortened firing intervals (Henson & Rugg, 2003) and accelerated peak latencies at stable durations of neuronal processing (Noguchi et al., 2004).

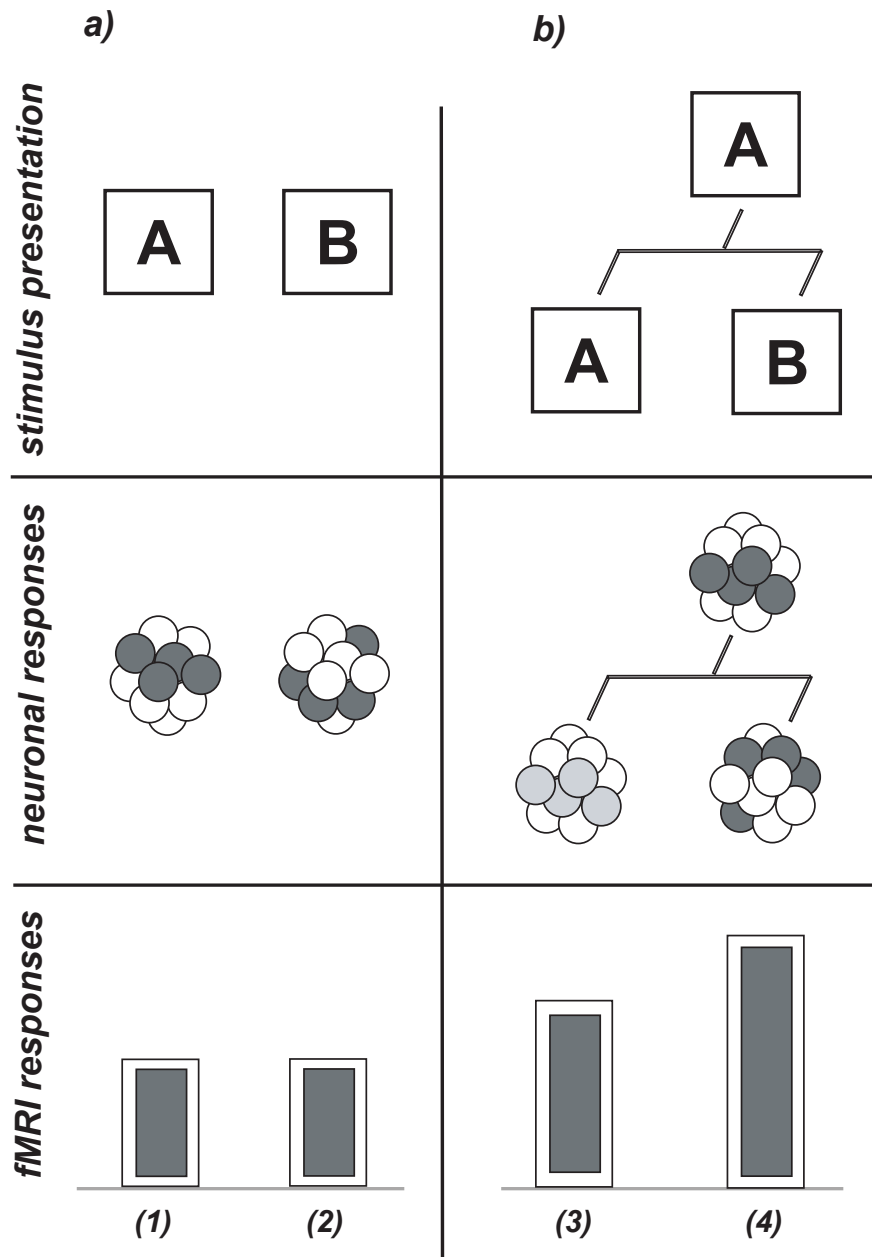


Figure 1.5: a) Conventional fMRI: Within a cluster of voxels, different neural population encode different stimulus properties, but result possibly in equally strong fMRI responses; (1) neuronal and fMRI response evoked by stimulus A, (2) neuronal and fMRI response evoked by stimulus B. b) fMRI adaptation: fMRI adaptation focuses on decreased neuronal responses to identical compared to different stimuli properties that are likely encoded by different neuronal populations allowing the investigation of functional at increased spatial resolution; (3) adapted neuronal and fMRI response evoked by repeated presentation of stimulus A, (4) neuronal and fMRI response evoked by consecutive presentation of stimulus A and B.

### 1.3.5 Principles of magnetoencephalography

Magnetoencephalography (MEG) is a suitable non-invasive technique for the investigation of functional properties of the human brain at high temporal resolution and has first been described by Cohen (1968). In general, changes in electrical currents generate a magnetic field perpendicular to their direction of flow. This principle is also applied in the electrically active nervous system. In contrast to Electroencephalography (EEG), that detects changes in electrical currents, MEG is sensitive to the detection of changes in the by electrical currents accompanied induced magnetic field. In detail, the highly organized pyramidal cells as well as their dendrites and axons establish a negative potential of around 70 mV within the cells. Neuronal firing elicits a change in this negative transmembrane potential resulting in the depolarization of the pyramidal cells followed by a current flow through the dendrites. This current flow shows a direction approximately perpendicular to the surface of the cortex and can therefore be either tangential or radial to the surface of the scalp depending on the location of the current in a sulcus or gyrus. The currents in a sulcus tangential to the surface of the scalp produce magnetic fields detectable from the surface of the scalp by superconducting quantum interference devices (SQUIDs). These SQUIDs are located radially to the head and are capable of detecting small magnetic fields in the range of pT ( $10^{-12}$  T).

### 1.3.6 Spatial encoding in MEG

Over the past twenty years, the number of SQUIDs has increased from single devices to as many as a few hundred providing a better understanding of the temporal activity in the human brain at different locations. However, the magnetic fields recorded on the surface of the scalp contain information about the distribution and direction of electrical activity within the entire brain, that can be referred back to the location of its origin by using dipole fitting methods. Several constraints must be made for such dipole analysis: Most importantly, the magnetic fields are recorded from a two-dimensional surface of the scalp, while electrical



activity occurs in a three-dimensional space within the brain. As a consequence of this technical limitation results a non-unique field inversion problem. Therefore, additional physiological knowledge (e.g. imaging techniques) or mathematical models need to be supplemented. Amongst these considerations is the assumption that the activation of a large number of cells is spatially small and modeled by a point equivalent dipole (Kaufman et al., 1981). To overcome these restrictions, recent studies (Liu et al., 2000, 2002; Downing et al., 2001) introduced an analysis that focuses on the signal of single SQUIDS rather than the modeling of dipoles from complex magnetic field. Other approaches have investigated oscillatory activation of neurons (Kristeva-Feige et al., 1993; Pantev, 1995; Pulvermuller et al., 1995).

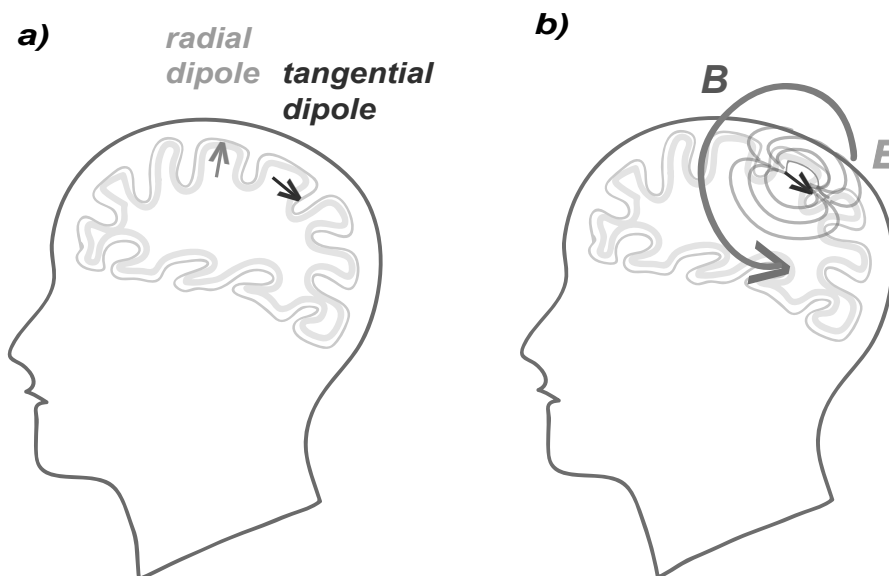


Figure 1.6: Pyramidal cells of the cortex generate a dendritic current flow perpendicular to the surface of the cortex. a) Current flow and dipole location: The resulting dipole is located radial to the scalp surface, if the current is located in a gyrus and vice versa. b) Dipole location and magnetic field: Tangential dipoles produce a magnetic field  $B$ , that can be detected by MEG.

### 1.3.7 Combined fMRI and MEG investigation

fMRI provides moderate spatial resolution, but poor temporal resolution. In contrast, MEG has an excellent temporal resolution at medium spatial resolution. While standard fMRI with its spatial resolution in the range of millimeters (Menon et al., 1999) cannot reach the unique spatial resolution of electrophysiology at the level of single cells, fMRI adaptation has been established to overcome this restriction in the spatial resolution of standard fMRI. Thus, the combination of fMRI adaptation and MEG enables the investigation at high spatial as well as temporal resolution.

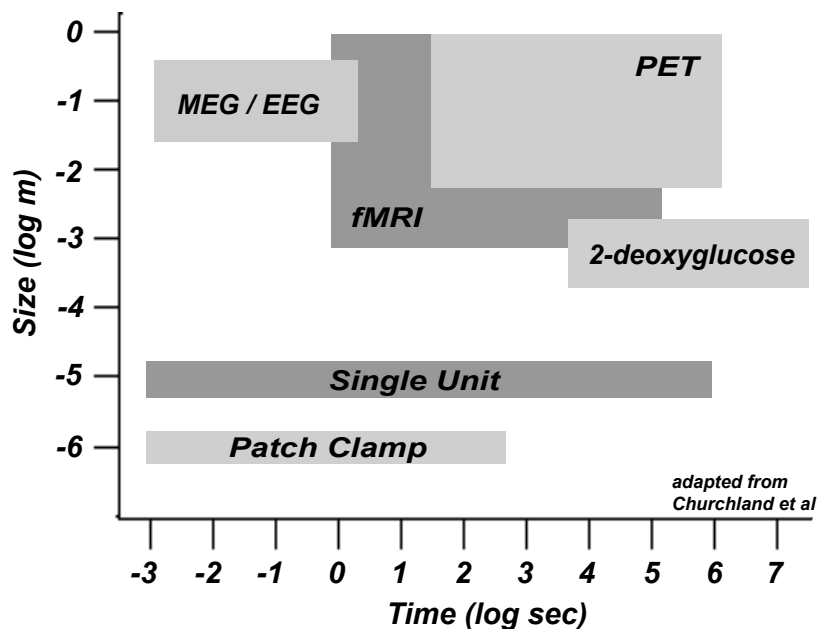


Figure 1.7: Spatial and temporal resolution of common neurophysiological methods: MEG = magnetoencephalography, EEG = electroencephalography, fMRI = functional magnetic resonance imaging, PET = positron emission tomography.

## 1.4 Purpose of investigation

The present experiments aimed at investigating the spatiotemporal characteristics of early and higher visual areas in the analysis of shape information at different temporal (variation in the stimulus presentation rates) and spatial (global shape vs. local features) scales. The experiments were conducted in the context of previous studies (Altmann et al., 2003; Kourtzi et al., 2003b), that provided evidence for the involvement of both higher visual areas such as the lateral occipital complex (LOC) - a region in the lateral occipital cortex, that extends anterior in to the temporal cortex and is thought to play a critical role in object recognition (Malach et al., 1995; Kanwisher et al., 1996; Grill-Spector et al., 2000) - and also early visual areas along the ventral visual pathway (V1, V2, VP, V4), whose cells were traditionally believed to function as local edge and line processors, in the analysis of global shape information.

The combination of human fMRI and MEG allowed the non-invasive investigation at high temporal and spatial resolution. Two fMRI studies (Experiment 1 and 2) tested the sensitivity to changes in the global shape across early and higher visual areas at different temporal scales by manipulating the temporal interval consecutively presented stimuli. Hereby, Experiment 2 controlled for attentional confounds of Experiment 1 and used a modified attentional task while the presentation paradigm remained unchanged. In addition, the temporal characteristics of shape processing were tested in a MEG study (Experiment 3) at high temporal resolution. Further, a third fMRI study (Experiment 4) investigated the processing of shape information at different spatial scales by testing the sensitivity to changes in the orientation of local features or changes in the global shape. A final fMRI study (Experiment 5) tested the sensitivity to changes in the local orientation of a random field of local features.

To address these questions, an event-related adaptation paradigm was employed, that focused on decreased responses for the repeated presentation of the same compared to different stimulus properties (Kourtzi & Kanwisher, 2000, 2001). The applied stimuli consisted of global shapes that were rendered by Gabor elements

aligned along the contour of the shape (Experiment 1 to 4) and yield the perception of global shapes as a result of the integration of these oriented local elements into global configurations (Field et al., 1993; Kovacs & Julesz, 1993, 1994; Hess et al., 2003). Further, arrays of randomly oriented Gabor elements (Experiment 5) were used.

The findings showed sensitivity to changes of the global shape in early and higher visual areas suggesting an involvement of these areas in the analysis of shape information. However, the differences of their spatiotemporal properties indicated a differential contribution of early and higher visual areas in shape processing. In detail, early visual areas encode local shape information in a transient manner, whereas higher visual areas are involved in sustained processing of the global shape. Further, the findings suggested a role of attention in the integration processes of early and higher visual areas. That is, occipitotemporal areas require attention to global shapes for sustained shape processing and in contrast, attention to local elements enhances their integration in early visual areas. Finally, the findings of the MEG study further improved our understanding of the temporal characteristics of shape processing underlying adaptation.

# Chapter 2

## Methods and Material

### 2.1 Observers

Fifteen observers participated in Experiment 1 (fMRI adaptation study) and ten observers in Experiment 2 (fMRI attentional control study of Experiment 1). Thirteen of the observers of Experiment 1 participated also in Experiment 3 (MEG adaptation study). Finally, fifteen observers took part in Experiment 4 (global / local adaptation study) and ten observers in Experiment 5 (orientation control study). Four observers in Experiment 1 and three observers in Experiment 4 were excluded from the analysis due to excessive head movement and one observer from Experiment 3 due to blinks in the majority of the trials. All observers had normal or corrected to normal vision, were paid for participation and gave their informed consent.

### 2.2 Visual stimuli

#### 2.2.1 Visual stimuli for Experiments 1 to 3

Observers were presented with shapes that consisted of Gabor elements (oriented sinusoidal luminance features with Gaussian envelopes that model roughly the RF structure of V1 simple cells) oriented collinearly along the contour of the

shape as as described in previous studies (Kovacs, 1996; Kovacs et al., 1999; Altmann et al., 2003; Kourtzi et al., 2003b). The shapes covered an average area of  $6.0^\circ \times 6.0^\circ$  and were presented in a gray background. In Experiment 1 and 2, seventy-eight different shapes (Figure 2.1) were used with a Gabor size of  $0.25^\circ$  and a distance of  $0.30^\circ$  visual angle between two neighboring Gabor elements. The size of a single Gabor element was defined as the area one standard deviation of the sinusoidal function around the center of a Gabor element. Further, the angle between two neighboring Gabor elements was calculated as the angle between the centers of these Gabor elements. Additionally, the mean overlap of all seventy-eight shapes was calculated as the mean percentual overlap of all possible combinations of two shapes including an area of  $1.0^\circ$  (approximate size of receptive fields in V1 at an eccentricity of  $6.0^\circ$ ) on both sides of a contour. This analysis revealed an average overlap of 72.20 % suggesting only small differences in the position between individual shapes. In Experiment 3, a subset of thirty-two of the seventy-eight shapes used in Experiment 1 and 2 were presented.

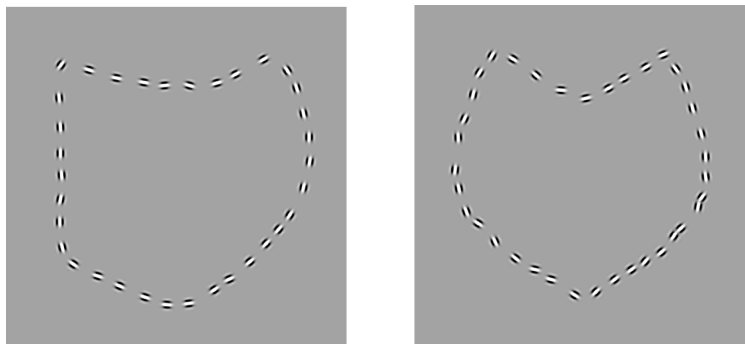


Figure 2.1: Sample stimuli of Experiment 1 to 3: The shapes consisted of Gabor elements oriented collinearly along the contour of the shape and were presented in a gray background. The shapes covered an average area of  $6.0^\circ \times 6.0^\circ$ .

### 2.2.2 Visual stimuli for Experiment 4

In parallel to Experiment 1 to 3, observers were presented with shapes that consisted of Gabor elements. However, the Gabor elements of individual shapes showed the same orientation and were presented at one of twelve different orientations ( $0^\circ$ ,  $15^\circ$ ,  $30^\circ$ ,  $45^\circ$ ,  $60^\circ$ ,  $75^\circ$ ,  $90^\circ$ ,  $105^\circ$ ,  $120^\circ$ ,  $135^\circ$ ,  $150^\circ$ ,  $165^\circ$  clockwise from vertical axis). The shapes covered an average area of  $8.9^\circ \times 8.9^\circ$  and were presented in a gray background. We used twenty-four different shapes (each at the twelve different orientations) with a Gabor size of  $0.5^\circ$  and an angle of  $0.5^\circ$  between two neighboring Gabor elements (identical stimulus properties were used in previous studies by Kourtzi et al., 2003b). Additionally, the shapes were symmetrical to an axis that was rotated around the center of the stimulus in steps of  $30^\circ$  and presented at six different positions ( $15^\circ$ ,  $45^\circ$ ,  $75^\circ$ ,  $105^\circ$ ,  $135^\circ$ ,  $165^\circ$  clockwise from vertical axis). By excluding vertical and horizontal orientations of the symmetry axis, we aimed at avoiding advantages for these orientations (Figure 2.3). In summary, 1728 different stimuli (twenty-four shapes, each presented at twelve orientations of Gabor elements and six rotations around the center of the stimulus) were employed in Experiment 4.

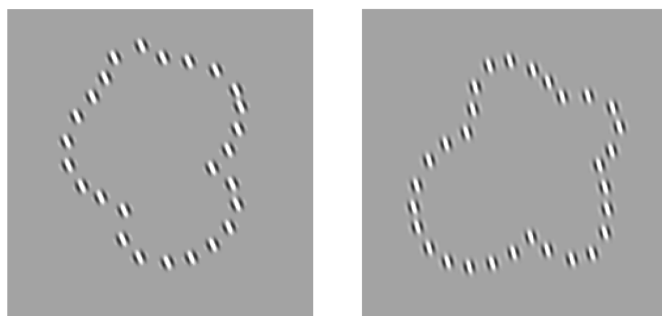


Figure 2.2: Sample stimuli of Experiment 4: The shapes consisted of identically oriented Gabor elements and were presented in a gray background. The Gabor elements were presented at twelve different orientations. Additionally, the symmetry axis of the shape was rotated around the center of the stimulus and presented at six different orientations. The shapes covered an average area of  $8.9^\circ \times 8.9^\circ$ .

### 2.2.3 Visual stimuli for Experiment 5

Observers were presented with a random field of Gabor elements (Figure 2.3) presented in a gray background. The Gabor elements had a size of  $0.5^\circ$  and an angle of  $0.5^\circ$  between two neighboring Gabor elements (stimulus properties identical to Experiment 4). The 96 random fields of Gabor elements covered an area of  $14.4^\circ \times 14.4^\circ$  and were arranged in pairs of two, that differed in the orientation of all local Gabor elements by  $90^\circ$ , while the position of the Gabor elements within the random field remained unchanged. That is, we used 192 different fields of random Gabor elements.

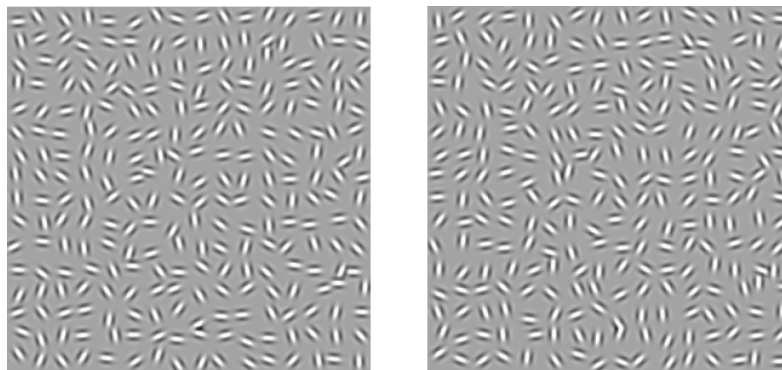


Figure 2.3: Sample stimuli of Experiment 5: The stimuli consisted of a random field of Gabor elements presented in a gray background. The Gabor fields were arranged in pairs that differed in the orientation of all local Gabor elements by  $90^\circ$  while the position of the Gabor elements remained unchanged. The stimuli covered an area of  $14.4^\circ \times 14.4^\circ$ .

### 2.2.4 Visual stimuli for LOC localizer

For the LOC localizer scans, grayscale images of novel and familiar objects as well as scrambled versions of each set were used (Kourtzi & Kanwisher, 2001). Twenty different stimuli were applied for each condition (Novel Intact, Familiar Intact, Novel Scrambled, Familiar Scrambled). The stimuli covered an area of



14.6° x 14.6°. In order to keep the low level features similar across conditions, an 18 x 18 grid was superimposed on all images. Scrambled versions of the intact images showed a change in the position of individual grid elements. Hereby, the grid elements around the center of the stimulus remained at central positions. In parallel, the grid elements in the periphery were placed at peripheral locations in the scrambled versions.

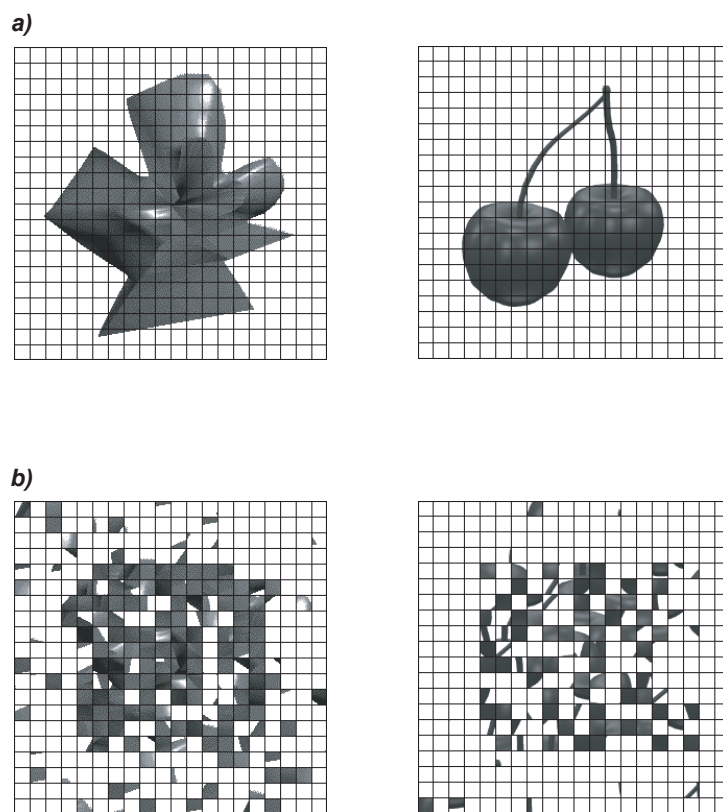


Figure 2.4: Sample stimuli of the LOC localizer for a) intact images of novel (left) and familiar (right) grayscale objects and b) scrambled versions of the novel (left) and familiar (right) grayscale objects displayed in a).

## 2.2.5 Visual stimuli for localizers of retinotopic areas

For the localizer scans of the early retinotopic areas located around the calcarine fissure, triangular wedge stimuli were employed to map the borders. The triangular wedge stimuli consisted of either gray-level natural images or black and white objects-from-texture and were presented at eight different rotational positions around the center of the stimulus as described in previous studies (Grill-Spector et al., 1998a). All stimuli covered an area of  $16.5^\circ \times 16.5^\circ$ . For the eccentricity mapping of the early retinotopic areas, concentric rings were used and presented at eight different eccentricities. In parallel to the triangular wedge stimuli, the ring stimuli consisted of either gray-level natural images or black and white objects-from-texture (Grill-Spector et al., 1998a). The stimuli covered areas between  $4.5^\circ \times 4.5^\circ$  for the smallest ring and  $16.5^\circ \times 16.5^\circ$  for the largest ring.

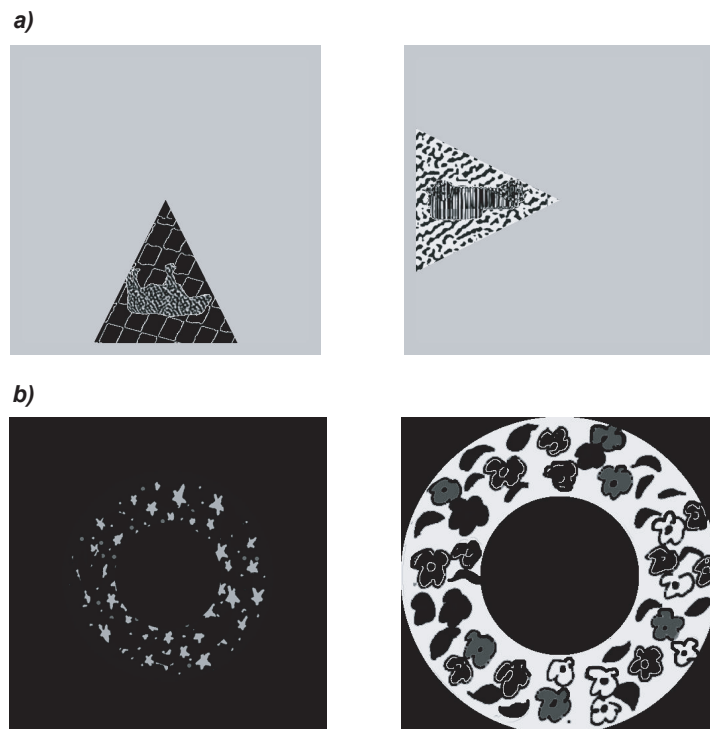


Figure 2.5: Sample stimuli of the retinotopic localizers for a) the border-mapping of the early retinotopic areas along the ventral visual pathway (V1, V, VP, V4) and b) their eccentricity mapping.

## 2.3 Design and task

### 2.3.1 General structure

All fMRI studies (Experiment 1, 2, 4 and 5) consisted of four event-related scans as well as two LOC localizer scans and the two localizer scans for the early retinotopic areas. In Experiment 3, two event-related recordings as well as one LOC localizer recording were conducted. The order of the scans was counterbalanced across observers. Before the start of the experiment, observers participated in a practice session, during which they were familiarized with the different types of stimuli and tasks.

### 2.3.2 Design and task for Experiment 1 and 2

An event-related adaptation paradigm (Buckner et al., 1998; Grill-Spector et al., 1999; Kourtzi et al., 2003a) was applied, in which sequential presentation of two identical shapes in a trial results in decreased fMRI responses compared to the presentation of two different shapes. The event-related scans included one hundred experimental trials (four conditions, twenty-five trials per condition and scan) and twenty-five fixation trials interleaved plus a sixteen-second fixation epoch at the beginning and an eight-second fixation epoch at the end of the scan. The order of trials was counterbalanced, so that trials from each condition, including the fixation condition, were preceded (2 trials back) equally often by trials from each of the other conditions as described in previous studies (Kourtzi & Kanwisher, 2000, 2001; Kourtzi et al., 2003a). Trials had a duration of three seconds. The two stimuli of a trial were presented consecutively (identical vs. different shapes) for 300 msec each. In order to study the temporal properties of shape processing across visual areas, the interstimulus interval (ISI) between the two stimuli of a trial was manipulated (Short ISI: 100 msec; Long ISI: 400 msec). Thus, the experiment consisted of four conditions (Figure 2.6): 1) Identical Shape / Short ISI, 2) Different Shape / Short ISI, 3) Identical Shape / Long ISI, and 4) Different Shape / Long ISI. The presentation of the stimuli was followed by a blank period

(Short ISI: 2300 msec; Long ISI: 2000 msec) before the onset of the next trial, in which the observers performed a two-alternative-forced-choice (2AFC) task. In Experiment 1, the observers were engaged in a matching task. That is, they reported whether the two consecutively presented shapes were identical or different (Same Shape, Different Shape). In contrast, the observers were instructed to perform a dimming task (detect luminance changes) on the fixation presented at the center of the display in Experiment 2. During this blank period and the ISI between the two stimuli of a trial, a central fixation cross appeared on the screen. Subjects were instructed to maintain fixation throughout the experimental scans.

### 2.3.3 Design and task for Experiment 3

The design and task for Experiment 3 was identical to Experiment 1. However, fixation trials were not included in this experiment.

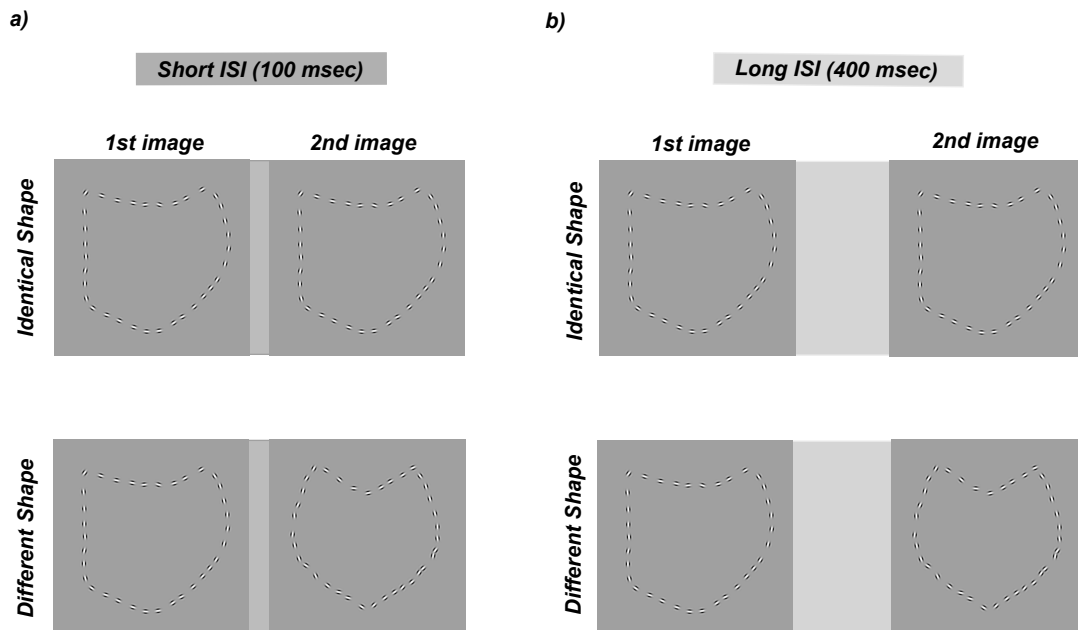


Figure 2.6: Design for Experiment 1 to 3: An event-related adaptation paradigm was applied. The ISI between the two stimuli of a trial was manipulated (Short ISI: 100 msec; Long ISI: 400 msec). This procedure results for a) the Short ISI in Identical Shape / Short ISI or Different Shape / Short ISI, and b) the Long ISI in Identical Shape / Long ISI or Different Shape / Long ISI.

### **2.3.4 Design and task for Experiment 4**

In parallel to Experiment 1, an adaptation paradigm was applied in this experiment.

Each trial had a duration of three seconds and consisted of two stimuli presented consecutively for 300 msec each with an ISI of 65 msec. In order to study the spatial properties of shape processing across early and higher visual areas, either the orientation of the local Gabor elements was manipulated by 90 degrees, while the global shape remained identical (Local Change); the global shape changed, while the orientation of the Gabor elements remained identical (Global Change); or both, local orientation and global shape were manipulated (Local / Global Change). Importantly, a change in the global shape was always associated with a change in the symmetry axis of the shape by 90 degrees. Thus, the experiment consisted of four conditions: a) Identical, b) Local Change, c) Global Change, and d) Local / Global Change. The presentation of the stimuli was followed by a blank period of 2335 msec before the onset of the next trial, in which a central fixation cross appeared on the screen and the observers responded to a 2AFC task.

### **2.3.5 Design and task for Experiment 5**

We used an event-related adaptation paradigm similar to Experiment 1. A number of ninety-six experimental trials (three conditions, thirty-two trials per condition and scan) and thirty-two fixation trials were tested per scan.

Trials had a duration of three seconds and consisted of either a single stimulus presentation, in which the second stimulus of a trial was not presented and a single stimulus was presented at the beginning of each trial, or two stimuli presented consecutively. Each stimulus was presented for 300 msec with an ISI of 100 msec in the trials consisting of two stimuli two stimuli. In these trials, we manipulated the orientation of the local Gabor elements by ninety degrees (Identical Orientation vs. Different Orientation). Thus the experiment consisted of three conditions: a) Single Presentation b) Repeated Presentation / Identical Orientation, and c) Repeated Presentation / Different Orientation. The presentation of the stimuli

was followed by a blank period (Single Presentation: 2700 msec; Repeated Presentation: 2300 msec) the onset of the next trial, in which a central fixation cross appeared on the screen.

Observers were instructed to perform a dimming task (detect luminance changes) on the fixation presented at the center of the display.

### **2.3.6 Design and task for localizer scans**

For the LOC localizer scans, each stimulus condition (Novel Intact, Familiar Intact, Novel Scrambled, Familiar Scrambled) was presented in a sixteen-second stimulus epoch (blocked design). Each condition was repeated four times with interleaved fixation periods. The blocked design balanced for the order of the conditions (Malach et al., 1995; Kanwisher et al., 1996). In a single block, twenty images were presented; each for 300 ms with a blank interval of 500 msec between images.

The observers were instructed to perform a 1-back matching task, that engaged their attention on all the stimulus types, i.e. the intact and the scrambled images of objects.

For the localizer scans of the early retinotopic regions, eight wedge positions and eight eccentricity levels for the rings were presented each for eight seconds and repeated eight times.

The observers were instructed to perform a dimming task (detect luminance changes) on the fixation presented at the center of the display.

## **2.4 Data acquisition**

Experiment 1 was conducted at a 1.5 Tesla Siemens scanner and Experiment 2, 4 and 5 at a 3 Tesla Siemens scanner located at the University Clinics, Tübingen. Data were collected with a head coil from 11 axial ( $3 \times 3 \times 5 \text{ mm}^3$ ) slices covering the occipital and temporal lobe. A Gradient Echo pulse sequence (TR = 1 sec,

TE = 40 msec for the event-related scans; TR = 2 sec, TE = 90msec for the localizer scans) was used. Experiment 3 was conducted at a 151-channel whole head MEG-system (CTF Inc., model: Omega) located at the University Clinics, Tübingen. The MEG sampling rate was 312.5 Hz. To control for head motion, the head position was acquired before and after each run using 3 separate localization coils (nasion, left and right preauricular). Runs, that showed movement larger than 5 mm were repeated.

## 2.5 Data analysis

### 2.5.1 General structure for fMRI data

fMRI data were processed using the Brain Voyager 4.9 software package. Pre-processing of all the functional data included head movement correction, temporal filtering of high frequencies, and removal of linear trends. The 2D functional images were aligned to 3D anatomical data and the complete data set was transformed to the standard coordinate system described by Talairach and Tournoux (1988). Anatomical data was additionally inflated and unfolded.

### 2.5.2 Regions of interest

The regions of interest (ROIs) individually defined for each observer (Figure 2.7 and 2.8) were the LOC and the early retinotopic areas along the ventral pathway (V1, V2, VP, V4). 3D statistical maps were calculated for an individual ROI by correlating the signal time course with a reference function for each voxel based on the hemodynamic response properties (Boynton et al., 1996; Cohen, 1997). The LOC was defined as the voxels in the ventral occipitotemporal cortex, that showed significantly stronger activation ( $p < 10^{-4}$ , corrected for multiple comparisons) to intact than scrambled images based on the averaged data of the two localizer scans. Two separate LOC subdivisions were identified as described in previous studies (e.g. Grill-Spector et al., 1999): the posterior lateral occipital region (LO)

and the anterior regions in the posterior fusiform gyrus (pFs). Early visual areas (V1, V2, VP, V4) were identified based on standard retinotopic mapping procedures (Engel et al, 1994; Sereno et al., 1995; DeYoe et al., 1996). Additionally, a subregion (between  $0^\circ$  and  $6.4^\circ$  in Experiment 1 and 2; and between  $0^\circ$  and  $9.0^\circ$  in Experiment 4) of areas V1, V2, VP and V4 was identified, that matched the area covered by the shapes displayed in the experimental stimuli.

<i>ROI</i>	<i>x</i>	<i>y</i>	<i>z</i>
<i>pFs, left</i>	<b>-32.96</b> (+/-3.61)	<b>-44.34</b> (+/-5.11)	<b>-15.19</b> (+/-2.81)
<i>LO, left</i>	<b>-37.78</b> (+/-2.20)	<b>-69.92</b> (+/-1.63)	<b>-14.06</b> (+/-5.47)
<i>pFs, right</i>	<b>30.69</b> (+/-4.03)	<b>-45.87</b> (+/-5.20)	<b>-15.10</b> (+/-2.71)
<i>LO, right</i>	<b>38.11</b> (+/-2.99)	<b>-67.89</b> (+/-5.16)	<b>-5.74</b> (+/-4.51)

Figure 2.7: Regions of Interest: Talairach coordinates for LO and pFs shown separately for each hemisphere. Displayed are the mean Talairach coordinates observed for the observers of Experiment 4. Similar coordinates were observed across experiments.



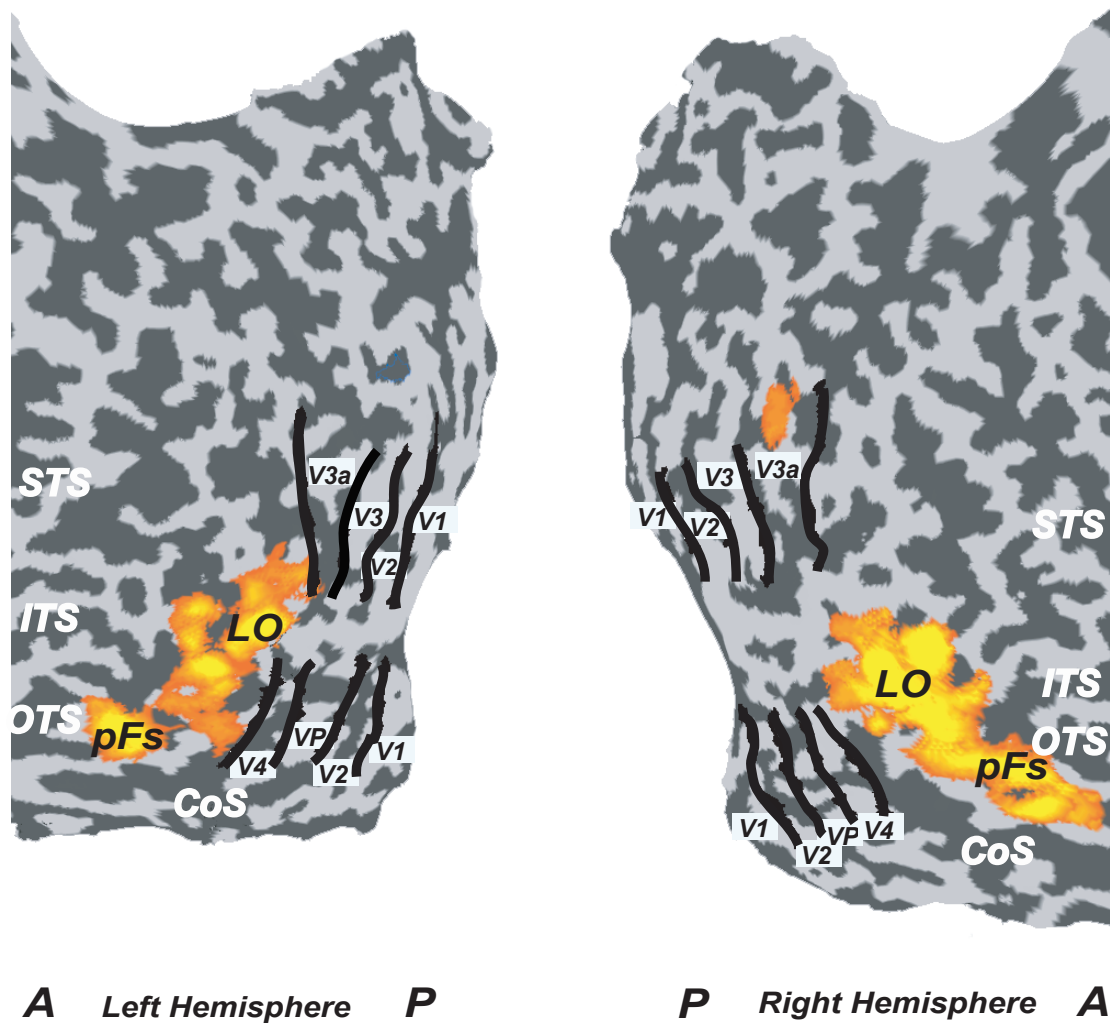


Figure 2.8: Activation Map: The activation map shows the LOC with its subdivisions LO and pFs in respect to the borders of retinotopic areas (V1, V2, V3, V3a, VP and V4) for one subject. The activation maps for the left and right hemisphere are projected on a flattened and unfolded cortical surface of an observer (A: anterior; P: posterior). The sulci are shown in dark gray and the gyri in light gray. Major sulci are marked as STS (superior temporal sulcus), ITS (inferior temporal sulcus), OTS (occipital temporal sulcus) and CoS (collateral sulcus). The LOC is defined as the voxels in the temporal and occipital lobe showing stronger activation to intact than scrambled images of familiar and novel graylevel images of objects. The borders of the retinotopic areas were defined based on standard retinotopic mapping procedures.

### 2.5.3 Timecourse analysis of fMRI data

fMRI responses were extracted by averaging the data of the event-related scans from all the voxels within each of the independently defined ROIs. For each scan, we averaged the signal intensity of all trials belonging to the same condition at each of the ten measurements (seconds) following stimulus presentation. Hereby the first measurement fell together with the onset of a trial. The percent signal change for each condition was calculated in relation to the fixation baseline as described in previous studies (Kourtzi & Kanwisher, 2000; 2001). Finally, the time courses were averaged across scans and observers.

It has been shown, that the largest differences across conditions occur at the peak of the hemodynamic response function several seconds after the onset of a stimulus (Boynton et al., 1996; Cohen et al., 1997). To identify the peak of the hemodynamic response function, an analysis of variance (ANOVA) was conducted for each experiment and ROI on the average of each of the 10 measurements from all observers with Measurement (Measurement 0 to Measurement 9) and Condition (Experiment 1 and 2: Identical Shape / Short ISI, Different Shape / Short ISI, Identical Shape / Long ISI, Different Shape / Long ISI; Experiment 4: Identical, Local Change, Global Change, Local / Global Change; Experiment 5: Single Presentation, Repeated Presentation / Identical Orientation, Repeated Presentation / Different Orientation) as independent factors. These ANOVAs showed a significant main effect of Measurement (e.g. pFs in Experiment 1:  $F [9, 90] = 44.20$ ,  $p < 0.001$ , pFs in Experiment 2:  $F [9, 81] = 4.24$ ,  $p < 0.001$ , pFs in Experiment 4:  $F [9, 99] = 41.31$ ,  $p < 0.001$ , and pFs in Experiment 5:  $F [9, 81] = 30.44$ ,  $p < 0.001$ ) and Condition (e.g. pFs in Experiment 1:  $F [3, 30] = 11.97$ ,  $p < 0.001$ , pFs in Experiment 2:  $F [3, 27] < 1$ ,  $p = 0.43$ , pFs in Experiment 4:  $F [3, 33] = 2.03$ ,  $p = 0.13$ , and pFs in Experiment 5:  $F [2, 81] = 5.69$ ,  $p = 0.01$ ) as well as a significant interaction between Measurement and Condition (e.g. pFs in Experiment 1:  $F [27,270] = 4.68$ ,  $p < 0.001$ , pFs in Experiment 2:  $F [27,243] = 3.06$ ,  $p < 0.001$ , pFs in Experiment 4:  $F [27,297] = 3.60$ ,  $p < 0.001$ , and pFs in Experiment 5:  $F [18, 162] = 3.68$ ,  $p < 0.001$ ) except for few testings. Contrast analysis revealed in the majority significant differences across conditions for Measurement

3 to 5 (e.g. pFs in Experiment 1 comparing Identical Shape / ISI 100ms versus Different Shape / ISI 400ms:  $F [27,270] = 20.88$ ,  $p = 0.001$  for Measurement 3,  $F [27,270] = 36.04$ ,  $p < 0.001$  for Measurement 4,  $F [27,270] = 17.73$ ,  $p < 0.001$  for Measurement 5; pFs in Experiment 2 comparing Identical Shape / ISI 100ms versus Different Shape / ISI 400ms:  $F[27,243] = 1.16$ ,  $p = 0.31$  for Measurement 3,  $F [27,243] = 4.63$ ,  $p = 0.06$  for Measurement 4,  $F [27,243] = 3.39$ ,  $p = 0.10$  for Measurement 5; pFs in Experiment 4 comparing Identical versus Local / Global Change:  $F[27,297] = 3.05$ ,  $p = 0.11$  for Measurement 3,  $F [27,297] = 6.59$ ,  $p < 0.05$  for Measurement 4,  $F [27,297] = 8.626$ ,  $p = 0.01$  for Measurement 5; pFs in Experiment 5 comparing Single Presentation versus Repeated Presentation / Different Orientation:  $F [18, 162] = 17.31$ ,  $p < 0.01$  for Measurement 3,  $F [18, 162] = 21.84$ ,  $p = 0.001$  for Measurement 4,  $F [18, 162] = 18.70$ ,  $p < 0.01$  for Measurement 5), but not for Measurement 0 (e.g. pFs in Experiment 1 comparing Identical Shape / ISI 100ms versus Different Shape / ISI 400ms:  $F [27,270] = 4.26$ ,  $p = 0.07$  for Measurement 0; pFs in Experiment 2 comparing Identical Shape / ISI 100ms versus Different Shape / ISI 400ms:  $F [27,243] < 1$ ,  $p = 0.79$  for Measurement 0; pFs in Experiment 4 comparing Identical versus Local / Global Change:  $F [27,297] < 1$ ,  $p = 0.71$  for Measurement 0; pFs in Experiment 5 comparing Single Presentation versus Repeated Presentation / Different Orientation:  $F [18, 162] < 1$ ,  $p = 0.99$  for Measurement 0). Similar findings were observed across ROIs and experiments.

Fitting a Gaussian model (Krugger & von Cramon, 1999) to the average fMRI responses across observers for each ROI separately showed an average peak of the hemodynamic response function at a mean latency across conditions of 4.33 sec (Identical Shape / ISI 100ms: 4.19 sec; Different Shape / ISI 100ms: 4.08 sec; Identical Shape / ISI 400ms: 4.62 sec; Different Shape / ISI 400ms: 4.41 sec) in the pFs for Experiment 1; a mean latency of 4.10 sec (Identical Shape / ISI 100ms: 4.00 sec; Different Shape / ISI 100ms: 4.08 sec; Identical Shape / ISI 400ms: 4.12 sec; Different Shape / ISI 400ms: 4.19 sec) in the pFs for Experiment 2; a mean latency of 4.21 sec (Identical: 4.11 sec; Local Change: 4.06 sec; Global Change: 4.36 sec; Local / Global Change: 4.30 sec) in the pFs

for Experiment 4; and a mean latency of 3.47 sec (Single Presentation: 3.21sec; Repeated Presentation / Identical Orientation: 3.63 sec; Repeated Presentation / Different Orientation: 3.58 sec) in the pFs for Experiment 5. Similar findings were observed across experiments and ROIs.

As a result of these analyses on the peak points of the hemodynamic response function, the average of the responses at Measurement 3 to 5 was taken as the measure of response magnitude for each condition in subsequent analyses.

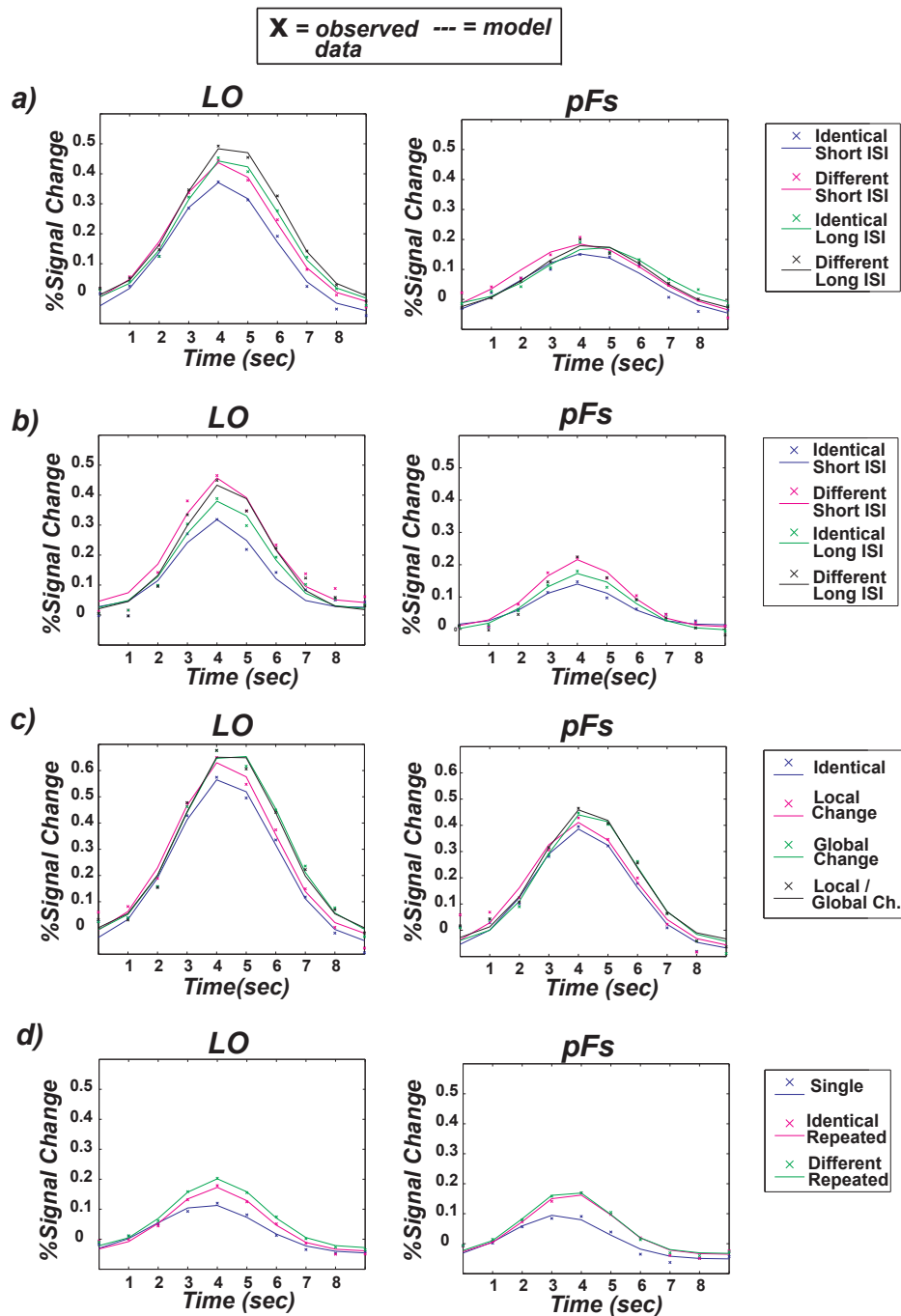


Figure 2.9: fMRI responses and fitted Gaussian model. Observed data for 10 different Measurements (in seconds from onset of trial) and fitted Gaussian model for LO and pFs for a) Experiment 1, b) Experiment 2, c) Experiment 4, and d) Experiment 5. The fits were conducted separately for each condition. Similar findings were observed for the remaining ROIs.

### 2.5.4 General structure for MEG data

MEG data were processed using the CTF software package, the BESA 2000 software package and custom-made in-house software. For the experimental recordings and the LOC localizer, data of each trial was analyzed 100 msec before the onset of the stimulus and until the offset of the stimulus. In detail, 700 msec were used for the analysis of the short ISI conditions, while an interval of 1000 msec was analyzed in the long ISI conditions and 400 msec for the LOC localizer. The complete set of data was adjusted to one head model by correcting positions with spherical spline interpolation individually for each observer. Preprocessing included the exclusion of trials from the analysis with amplitudes higher than 2.0 pT due to excessive eye blinking and filtering of the time series with a 30 Hz low-pass filter. The baseline was defined as the average of the responses for the 100 msec - interval before the beginning of each trial. Data was further averaged across runs and observers in relation to the baseline.

### 2.5.5 Field of Interest

A Field of Interest (FOI) analysis was performed in approach to the "Sensor of Interest" (SOI) analysis (Downing et al., 2001) and the "ROI" analysis applied to our fMRI data. In contrast to the SOI analysis, this method focused on the recordings of the complete magnetic field rather than single sensors. In parallel to the standard fMRI ROI analysis (Malach et al., 1995), the FOI for the LOC was defined based on stronger responses to intact than scrambled versions of objects. Hereby, we used the responses averaged across all observers. In order to specify these differences in space and time, we used the difference between the two conditions of the global field power (GFP) and specified the temporal interval with the maximum of the GFP. That is, we calculated the GFP as the root of the mean squared magnetic responses over all sensors as a function of time and then subtracted the GFP of the scrambled from the intact images for each recording. A difference in these GFPs higher than three times their standard deviation of the 100 msec baseline before the onset of the stimuli was defined as a statistically

significant difference between intact and scrambled images. Further, we specified the maximum of these differences over time as the temporally highest activity originating from the LOC. This analysis revealed a temporal interval of 256 msec after the onset of the stimuli (Figure 2.10). Additionally, we used the magnetic field revealed for the intact images at 256 msec (Figure 2.10) as the spatial distribution of a magnetic field with its origin in the LOC bilaterally and performed a dipole fit around a short interval using four dipoles: one dipole for each hemisphere representing the LOC and additional dipoles around the occipital pole and in the parietal lobe (covering feature processing and attentional demands). 78.12 % of the variance at this timepoint was explained by the two LOC dipoles. Finally, we performed a co-registration (BESA 2000, Brainvoyager 4.9) between the location of the LOC dipoles and the independently identified voxels for the LOC in our fMRI localizer (from individual observers), which suggested a high correlation between the locations of the LOC (Figure 2.10). That is, similar locations were defined as the LOC in both the MEG and the fMRI study.

### **2.5.6 Timecourse analysis of MEG data**

The LOC FOI was fitted to the complete data set of the experimental recordings by calculating a correlation index. This correlation index indicated the mean percentage over all sensors for the data of the experimental recordings at each temporal interval that can be explained by the LOC FOI. By definition, the index hereby was 1.0 in case the magnetic field and the LOC FOI were identical and -1.0 in case they were identical, except for opposite signs in all sensors. In contrast, an index of 0.0 indicated, that these fields were completely different from each other. For both ISIs, the correlation index for consecutively identical as well as different stimuli presented in a trial was calculated for each subject and then averaged across subjects. Further, t-tests at the level of  $p < 0.01$  on the differences for identical and different shapes in a trial independently for the two ISIs were conducted to specify the temporal intervals, that showed significant differences between conditions. In parallel to the fMRI-adaptation approach, adaptation was defined as a significant lower index for consecutively identical than different stimuli.

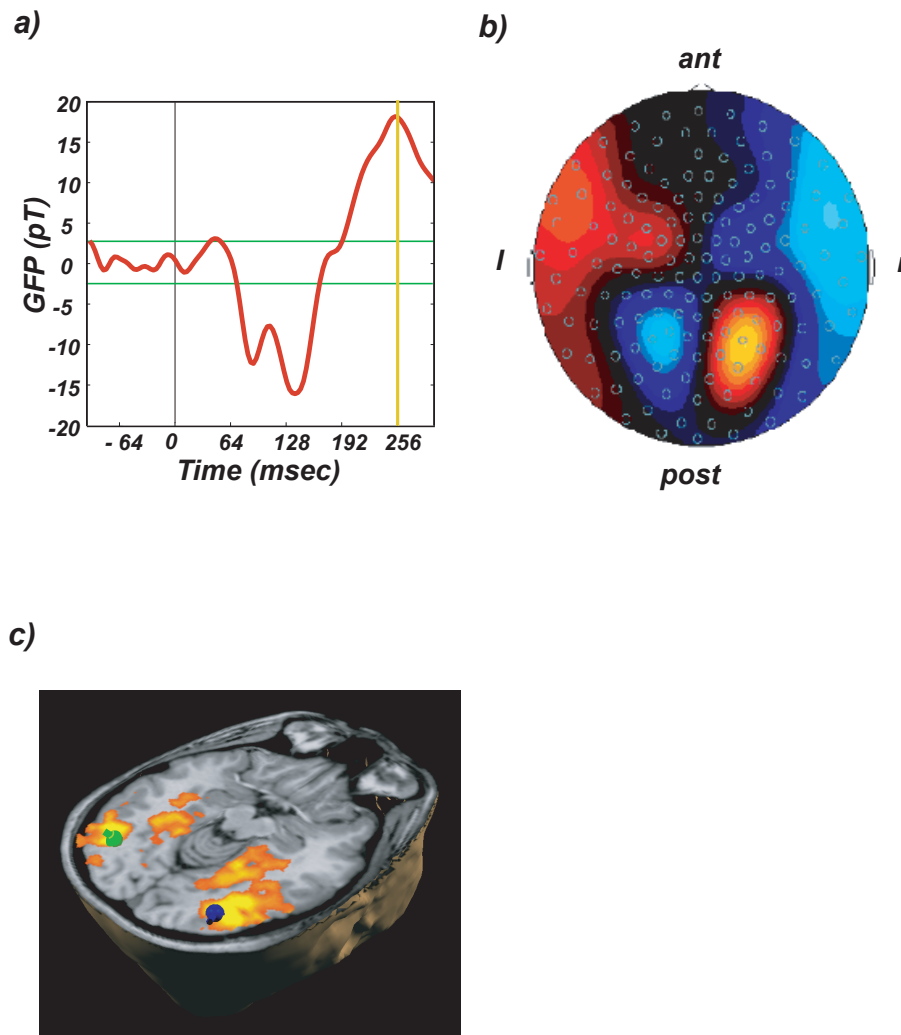


Figure 2.10: a) Differences for GFP of intact and scrambled images as a function of time (red). A difference in these GFPs higher than three times their standard deviation of the 100 msec baseline before the onset of the stimuli (green) was defined as a statistically significant difference between intact and scrambled images. The maximum of these differences revealed a temporal interval of 256 msec after the onset of the stimuli (yellow). b) Observed magnetic field for LOC localizer at a latency of 256 msec. ant. = anterior, post. = posterior c) Co-registration between the location of the LOC dipoles (marked in green and blue) and the independently identified voxels for the LOC (marked in yellow to red; one individual observer) suggested high correlation for the locations of the LOC. Similar results were observed across observers.



## 2.6 Psychophysical Data

### 2.6.1 General structure

We analyzed the psychophysical data of the matching tasks (Experiment 1, 3 and 5) by computing the mean performance as the percentage of correct responses in relation to all given responses for each condition averaged across observers and the mean reaction time as the time for each condition from the onset of the trial to the observers' key responses averaged across observers. Data of the dimming tasks (Experiment 2 and 4) was not acquired and could therefore not be analyzed.

### 2.6.2 Psychophysical Data for Experiment 1 and 3

All eleven observers of Experiment 1 responded correctly in 97.6 % of the trials (97.7 % for Identical Shape / Short ISI, 98.5 % for Different Shape / Short ISI, 95.9 % for Identical Shape / Long ISI and 98.3 % for Different Shape / Long ISI). Specifically, a repeated measures ANOVA with ISI (Short ISI, Long ISI) and Shape (Identical Shape, Different Shape) as independent factors showed no main effect for ISI ( $F [1,10] = 1.91, p = 0.20$ ) and Shape ( $F [1,10] = 2.01, p = 0.19$ ) indicating, that the observers were able to discriminate consecutively identical from different shapes with no differences between the short and long ISI. Further, observers showed a mean reaction time of 1.09 sec (1.07 sec for Identical Shape / Short ISI, 1.15 sec for Different Shape / Short ISI, 1.04 sec for Identical Shape / Long ISI and 1.10 sec for Different Shape / Long ISI). A repeated measures ANOVA with ISI (Short ISI, Long ISI) and Shape (Identical Shape, Different Shape) as independent factors showed no main effect for ISI ( $F [1, 10] = 2.39, p = 0.15$ ), but a main effect of Shape ( $F [1, 10] = 9.19, p < 0.05$ ). In accordance with previous reports (Schweitzer, 1991), this finding indicated faster reaction times for identical shapes than different shapes. Similar findings were observed for Experiment 3.

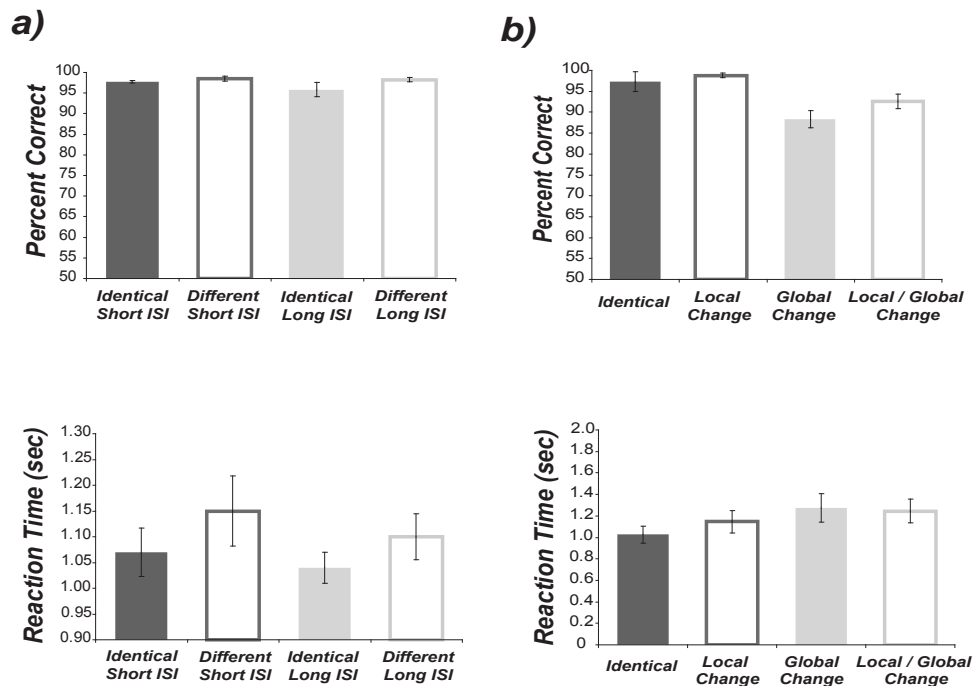


Figure 2.11: Psychophysical data. a) Experiment 1 ( $n = 11$ ) and b) Experiment 4 ( $n = 8$ ): Displayed is the mean performance (left) and reaction time (right) across conditions.

### 2.6.3 Psychophysical Data for Experiment 4

The psychophysical data of eight subjects was analyzed; data of four subjects could not be analyzed due to technical failure. Observers responded correctly in 94.3 % of the trials (97.3 % for Identical, 98.8 % for Local Change, 88.3 % for Global Change and 92.6 % for Local / Global Change). Specifically, a repeated measures ANOVA with Global Level (Identical Shape, Different Shape) and Local Level (Identical Orientation, Different Orientation) as independent factors showed a main effect for Global Level ( $F [1,7] = 12.00$ ,  $p = 0.01$ ) and Local Level ( $F [1,7] = 6.94$ ,  $p < 0.05$ ). No significant interaction between Global Level and Local Level ( $F [1,7] < 1$ ,  $p = 0.41$ ) was observed. That is, observers showed higher performance for identical than different shapes as well as different orientations of the local Gabor elements than identical orientations. Further, observers showed a mean reaction time of 1.18 sec (1.03 sec for Identical, 1.15 sec for Local Change, 1.27 sec for Global Change and 1.25 sec for Local / Global Change). A repeated measures ANOVA with Global Level (Identical Shape, Different Shape) and Local Level (Identical Orientation, Different Orientation) as independent factors showed

no main effect for Local Level ( $F [1, 7] = 2.54, p = 0.16$ ), but a main effect of Global Level ( $F [1, 7] = 12.85, p < 0.01$ ). That is, observers responded faster for identical than different shapes. Again, in accordance with previous reports (Schweitzer, 1991), this finding indicated faster reaction times for identical shapes than different shapes.

## 2.7 Eye-movement data

### 2.7.1 Eye-movement data for Experiment 1

Eye-movement recordings for three observers outside the scanner using an infrared camera system (Eyelink 2.02) showed no differences in the number and amplitude of saccades across conditions (including fixation). Specifically, a repeated measures ANOVA was conducted with Condition (Fixation, Short ISI / Identical Shape, Short ISI / Different Shape, Long ISI / Identical Shape, Long ISI / Different Shape) as independent factor over the number of saccades as well as their mean x - and y - amplitudes. No main effect of Condition was found for the number of saccades ( $F [4, 8] < 1, p = 0.67$ ) and the mean x - amplitude ( $F [4, 8] = 1.42, p = 0.31$ ). However, a main effect of Condition was found for the mean y - amplitude ( $F [4, 8] = 4.08, p = 0.04$ ). Additionally, a repeated measures ANOVA with Condition (Fixation, Short ISI / Identical Shape, Short ISI / Different Shape, Long ISI / Identical Shape, Long ISI / Different Shape) as independent factor over the mean x - and y - position (mean eye position) showed no main effect of Condition for the mean x - position ( $F [4, 8] = 1.22, p = 0.37$ ) and the mean y - position ( $F [4, 8] = 2.19, p = 0.16$ ). In summary, similar eye-movements were observed across conditions in Experiment 1.

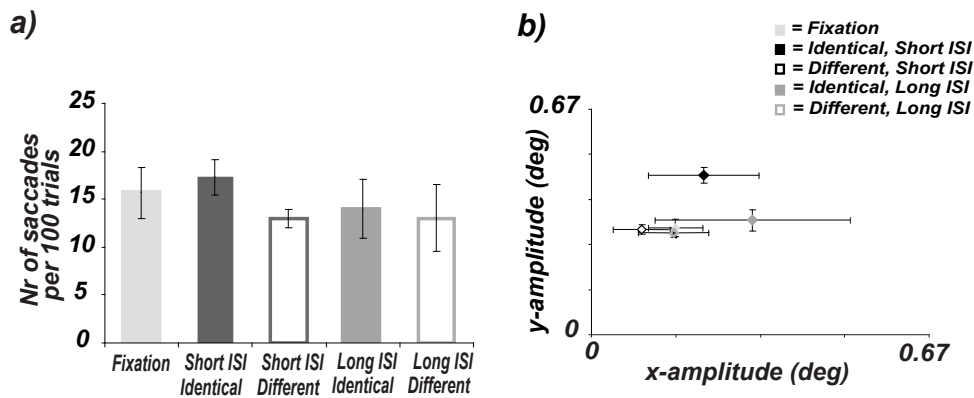


Figure 2.12: Eye-movement data for Experiment 1. Eye-movements were similar across conditions. a) Displayed are the average number of saccades across subjects for individual conditions ( $n = 3$ ). b) Displayed are the mean x - and y - amplitude of saccades averaged across subjects for individual conditions.

## 2.7.2 Eye-movement data for Experiment 2

Eye-movement recordings for three observers (observers of Experiment 1) outside the scanner using an infrared camera system (Eyelink 2.02) showed no differences in the number and the amplitude of saccades across conditions (including fixation). Specifically, a repeated measures ANOVA was conducted with (Fixation, Short ISI / Identical Shape, Short ISI / Different Shape, Long ISI / Identical Shape, Long ISI / Different Shape) as independent factor over the number of saccades as well as their mean x - and y - amplitudes. No main effect of Condition was found for the number of saccades ( $F [4, 8] = 1.17, p = 0.98$ ), the mean x - amplitude ( $F [4, 8] = 1.61, p = 0.26$ ) and the mean y - amplitude ( $F [4, 8] = 1.40, p = 0.32$ ). Additionally, a repeated measures ANOVA with Condition (Fixation, Short ISI / Identical Shape, Short ISI / Different Shape, Long ISI / Identical Shape, Long ISI / Different Shape) as independent factor over the mean x - and

y - position showed no main effect of Condition for the mean x - position ( $F [4, 8] < 1, p = 0.53$ ) and the mean y - position ( $F [4, 8] = 2.03, p = 0.18$ ). In summary, similar eye-movements were observed across conditions in Experiment 2.

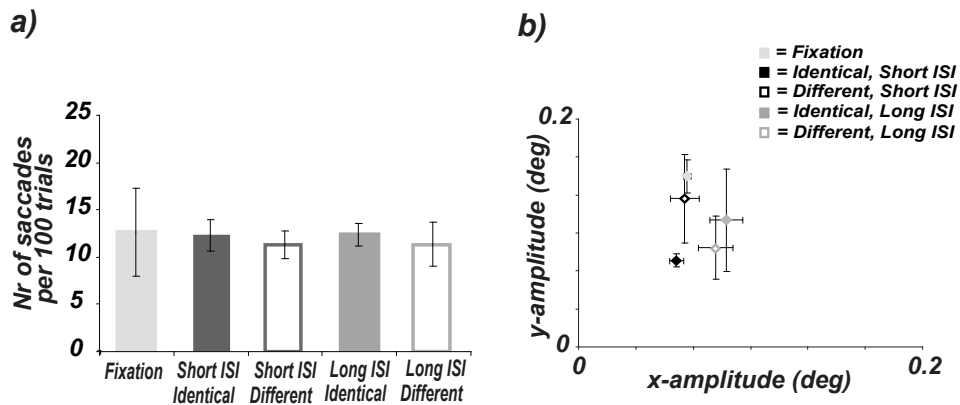


Figure 2.13: Eye-movement data for Experiment 2. Eye-movements were similar across conditions. a) Displayed are the average number of saccades across subjects for individual conditions ( $n = 3$ ). b) Displayed are the mean x - and y - amplitude of saccades averaged across subjects for individual conditions.

### 2.7.3 Comparison of eye-movement data for Experiment 1 & 2

Eye-movement data for Experiment 1 and 2 were compared by conducting a repeated measures ANOVA with Task (matching task, dimming task) and Condition (Fixation, Short ISI / Identical Shape, Short ISI / Different Shape, Long ISI / Identical Shape, Long ISI / Different Shape) as independent factors over the number of saccades, the mean x - and y - amplitude. No main effects of Task and Condition were found for the number of saccades (Task:  $F [1, 2] < 1, p = 0.45$ , Condition:  $F [4, 8] = 1.20, p = 0.38$ ), the mean x - amplitude (Task:  $F [1, 2] < 1, p = 0.33$ , Condition:  $F [4, 8] = 1.47, p = 0.30$ ) and the mean y - amplitude (Task:  $F [1, 2] < 1, p = 0.52$ , Condition:  $F [4, 8] < 1, p = 0.69$ ). Additionally, a repeated mea-

sures ANOVA with Task (matching task, dimming task) and with (Fixation, Short ISI / Identical Shape, Short ISI / Different Shape, Long ISI / Identical Shape, Long ISI / Different Shape) as independent factors over the mean x - and y - position showed no main effects of Task and Condition for the mean x - position (Task:  $F [1, 2] = 7.09, p = 0.12$ , Condition:  $F [4, 8] < 1, p = 0.48$ ) and the mean y - position (Task:  $F [1, 2] < 1, p = 0.45$ ), Condition:  $F [4, 8] = 2.64, p = 0.11$ ). In summary, similar eye-movements were observed across Experiment 1 and 2.

#### **2.7.4 Eye-movements for Experiment 4**

Eye-movement recordings for four observers outside the scanner using an infrared camera system (Eyelink 2.02) showed no differences in the number and the amplitude of saccades across conditions (including fixation). Specifically, a repeated measures ANOVA was conducted with Condition (Fixation, Identical, Local Change, Global Change, Local / Global Change) as independent factor over the number of saccades as well as their mean x - and y - amplitudes. No main effect of Condition was found for the number of saccades ( $F [4, 12] = 1.97, p = 0.16$ ), the mean x-amplitude ( $F [4, 12] = 1.77, p = 0.20$ ) and the mean y-amplitude ( $F [4, 12] < 1, p = 0.84$ ). Additionally, a repeated measures ANOVA with Condition (Fixation, Identical, Local Change, Global Change, Local / Global Change) as independent factor over the mean x - and y - position showed no main effect for Condition for the mean x - position ( $F [4, 12] < 1, p = 0.97$ ) and the mean y - position ( $F [4, 12] < 1, p = 0.81$ ). In summary, we observed similar eye-movement across conditions in Experiment 2.

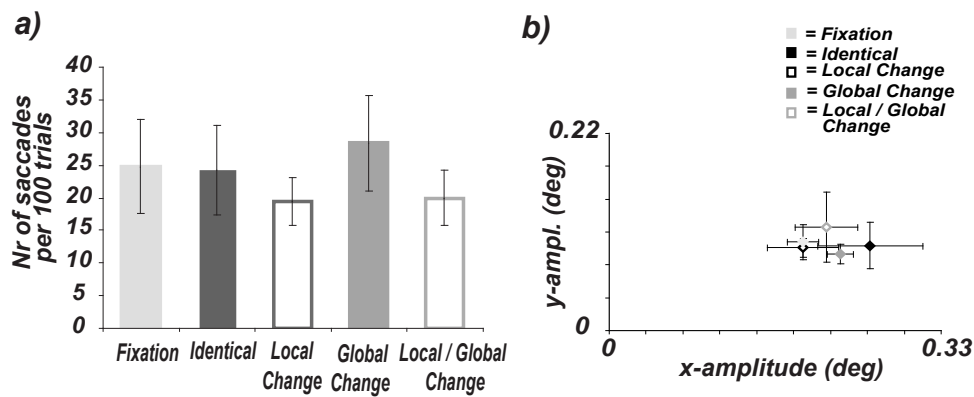


Figure 2.14: Eye-movement data for Experiment 4. Eye-movements were similar across conditions. a) Displayed are the average number of saccades across subjects for individual conditions ( $n = 4$ ). b) Displayed are the mean x - and y - amplitude of saccades averaged across subjects for individual conditions.

### 2.7.5 Eye-movements for Experiment 5

Eye-movement recordings for three observers outside the scanner using an infrared camera system (Eyelink 2.02) showed no differences in the number and the amplitude of saccades across conditions (including fixation). Specifically, a repeated measures ANOVA was conducted with Condition (Fixation, Repeated Presentation / Identical Orientation, Repeated Presentation / Different Orientation) as independent factor over the number of saccades, the mean x - and y - amplitude. No main effect of Condition was found for the number of saccades ( $F [3, 6] < 1, p = 0.63$ ), the mean x - amplitude ( $F [3, 6] = 1.390, p = 0.33$ ) and the mean y - amplitude ( $F [3, 6] = 1.37, p = 0.34$ ). Additionally, a repeated measures ANOVA with Condition (Fixation, Repeated Presentation / Identical Orientation, Repeated Presentation / Different Orientation) as independent factor over the mean x - and y - position showed no main effect for Condition for the mean

x - position ( $F [3, 6] = 2.19, p = 0.19$ ) and the mean y - position ( $F [3, 6] = 2.52, p = 0.15$ ). In summary, we observed similar eye-movement across conditions in Experiment 2.

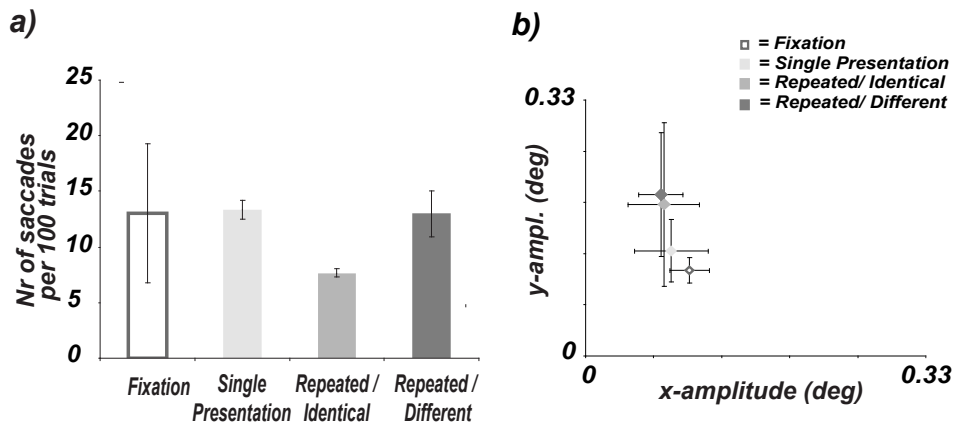


Figure 2.15: Eye-movement data for Experiment 5. Eye-movements were similar across conditions. a) Displayed are the average number of saccades across subjects for individual conditions ( $n = 3$ ). b) Displayed are the mean x - and y - amplitude of saccades averaged across subjects for individual conditions.



# Chapter 3

## Results

### 3.1 Results for Experiment 1

Experiment 1 aimed at testing the temporal characteristics of shape processing across visual areas by manipulating the temporal interval between the two consecutively stimuli presented in a trial. fMRI adaptation, that is lower responses for identical than different stimuli, was observed in early (V1, V2, VP, V4) and higher (LO, pFs) visual areas as reported previously (Kourtzi & Kanwisher, 2000, 2001; Kourtzi et al., 2003). Interestingly, these adaptation effects were observed only for the short ISI in early visual areas. In contrast, adaptation effects were observed for the short and long ISI in the subregions of the LOC.

Additionally, a repeated measures ANOVA with Shape (Identical Shape, Different Shape), ISI (Short ISI, Long ISI), and ROI (V1, V2, VP, V4, LO and pFs) as independent factors showed significant main effects of Shape ( $F [1, 10] = 8.77, p = 0.01$ ), ISI ( $F [1, 10] = 12.47, p < 0.01$ ) and ROI ( $F [5, 50] = 8.28, p < 0.01$ ). More importantly, significant interactions were observed of ROI and Shape ( $F ([5, 50] = 3.34, p = 0.01$ ) and ROI and ISI ( $F [5, 50] = 8.82, p < 0.01$ ). Contrast analysis revealed significant stronger responses for different than identical shapes for the short ISI in all ROIs: V1 ( $F [5,50] = 9.32, p < 0.01$ ), V2 ( $F [5,50] = 11.09, p < 0.01$ ), VP ( $F [5,50] = 11.96, p < 0.01$ ), V4 ( $F [5,50] = 3.74, p = 0.05$ ), LO ( $F [5,50] = 21.52, p < 0.01$ ) and pFs ( $F [5,50] = 12.10, p < 0.01$ ). Additionally,

significantly stronger responses for different than identical shapes for the long ISI were observed in LO ( $F [5,50] = 7.33, p < 0.01$ ) and pFs ( $F [5,50] = 5.40, p < 0.05$ ). However, these effects were not found in V1 ( $F [5,50] < 1, p = 0.54$ ), V2 ( $F [5,50] < 1, p = 0.75$ ), VP ( $F [5,50] < 1, p = 0.87$ ) and V4 ( $F [5,50] = 2.71, p = 0.11$ ).

In summary, adaptation effects for the short ISI were observed both in early and higher visual areas. In contrast, adaptation effects for the long ISI appeared only in higher, but not early visual areas. These findings are consistent with previous imaging studies, that showed stronger adaptation effects for shorter than longer ISIs (Huettel & McCarthy, 2001; Huettel et al., 2004), but further are in accordance with earlier neurophysiological studies, that reported adaptation effects for complex cells in V1 at an ISI below 200 msec (Müller et al., 1999). Thus, the present findings suggest a transient analysis of shape information in early visual areas compared to more sustained processing in higher visual areas.

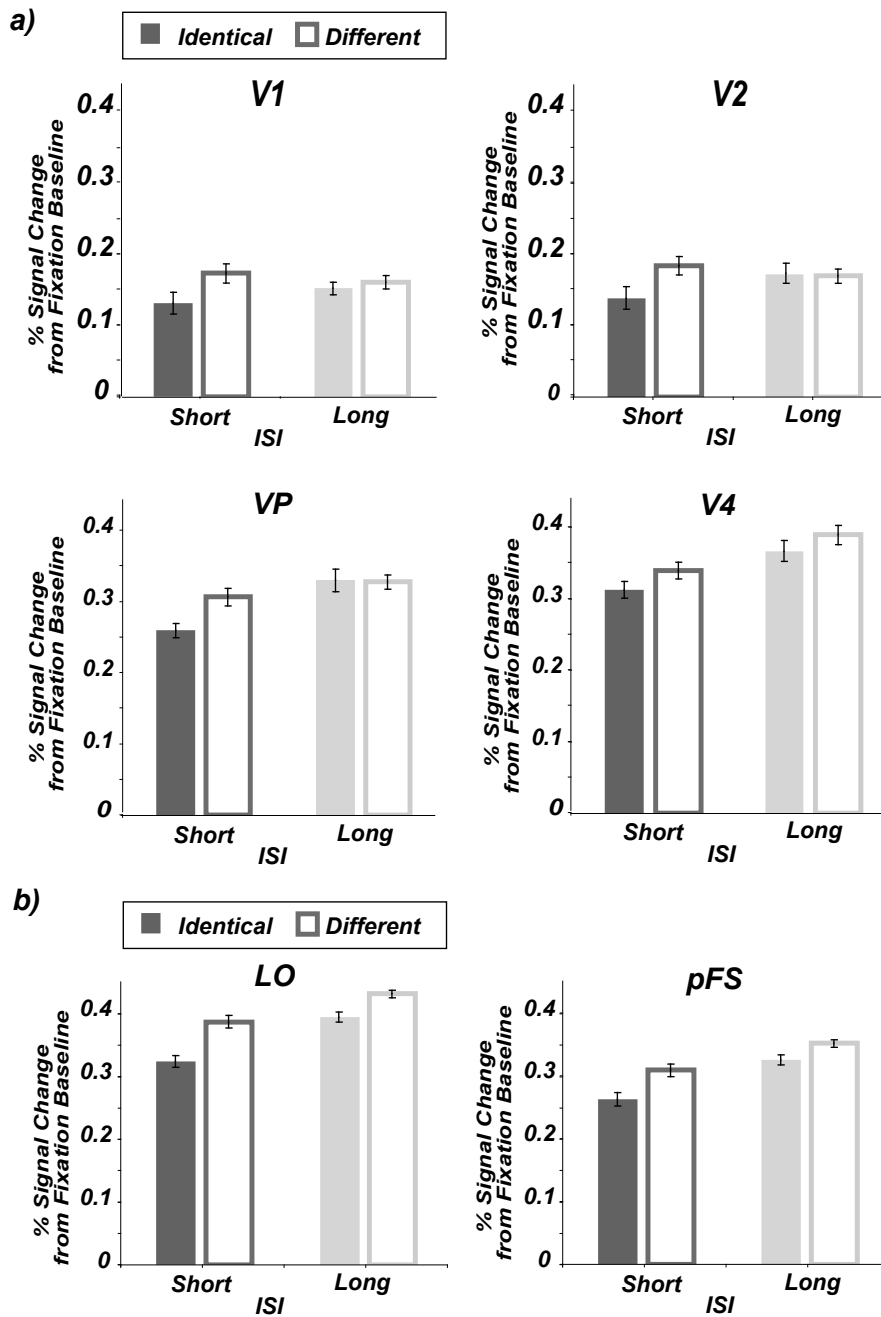


Figure 3.1: fMRI responses for Experiment 1. Displayed are the normalized responses in a) early visual areas along the ventral visual pathway (V1, V2, VP and V4) and b) the subdivisions of the LOC (LO and pFs). Responses were calculated as Percent Signal Change from Fixation Baseline. The mean percent signal change for all the conditions was subtracted from the mean percent signal change for each condition and finally the mean percent signal change for all conditions across subjects was added. Responses of one hundred trials per conditions were averaged across measurements (3 to 5 seconds after the onset of a trial) and subjects. Error bars indicate the standard error across subjects.

## 3.2 Results for Experiment 2

Experiment 2 controlled for attentional confounds of Experiment 1, in which observers might have paid less attention for identical shapes in a trial compared to trials with a change in the shape. Observers now performed a dimming task (detection of luminance changes) on the fixation cross presented at the center of the display.

Experiment 2 confirmed the results observed in Experiment 1. fMRI adaptation was observed in areas V2, VP, V4, LO and pFs. These adaptation effects appeared in all areas for the short ISI (100 msec), but not the long ISI (400 msec). Interestingly, no adaptation effects were observed in V1 neither for the short nor the long ISI.

Specifically, a repeated measures ANOVA with Shape (Identical Shape, Different Shape), ISI (Short ISI, Long ISI), and ROI (V1, V2, VP, V4, LO and pFs) as independent factors showed significant main effects of Shape ( $F [1, 9] = 18.97$ ,  $p < 0.01$ ) and ROI ( $F [5, 45] = 14.18$ ,  $p < 0.01$ ), but not ISI ( $F [1, 9] = 2.49$ ,  $p = 0.15$ ). A significant interaction of ROI and Shape ( $F [5, 45] = 3.35$ ,  $p = 0.01$ ) was observed. Contrast analysis showed significantly stronger responses for different than identical shapes for the short ISI in V2 ( $F [5, 45] = 10.24$ ,  $p < 0.01$ ), VP ( $F [5, 45] = 7.37$ ,  $p < 0.01$ ), V4 ( $F [5, 45] = 10.27$ ,  $p < 0.01$ ), LO ( $F [5, 45] = 15.43$ ,  $p < 0.01$ ) and pFs ( $F [5, 45] = 4.01$ ,  $p = 0.05$ ), but not in V1 ( $F [5, 45] < 1$ ,  $p = 0.60$ ). No significant differences between identical and different shapes were observed for the long ISI across ROIs: V1 ( $F [5, 45] = 1.13$ ,  $p = 0.29$ ), V2 ( $F [5, 45] < 1$ ,  $p = 0.36$ ), VP ( $F [5, 45] < 1$ ,  $p = 0.84$ ), V4 ( $F [5, 45] = 1.40$ ,  $p = 0.24$ ), LO ( $F [5, 45] = 2.06$ ,  $p = 0.16$ ) and pFs ( $F [5, 45] < 1$ ,  $p = 0.40$ ).

In summary, the findings of Experiment 2 indicate increased transient processing of global shape when the attention is focused away from the stimulus and suggest less sustained neural sensitivity under divided attention. Further, these findings are in accordance with previous studies (Eger et al., 2004; Murray & Wojciulik, 2004; Rezec et al., 2004) suggesting attentional modulation of psychophysical behavior and fMRI adaptation effects.

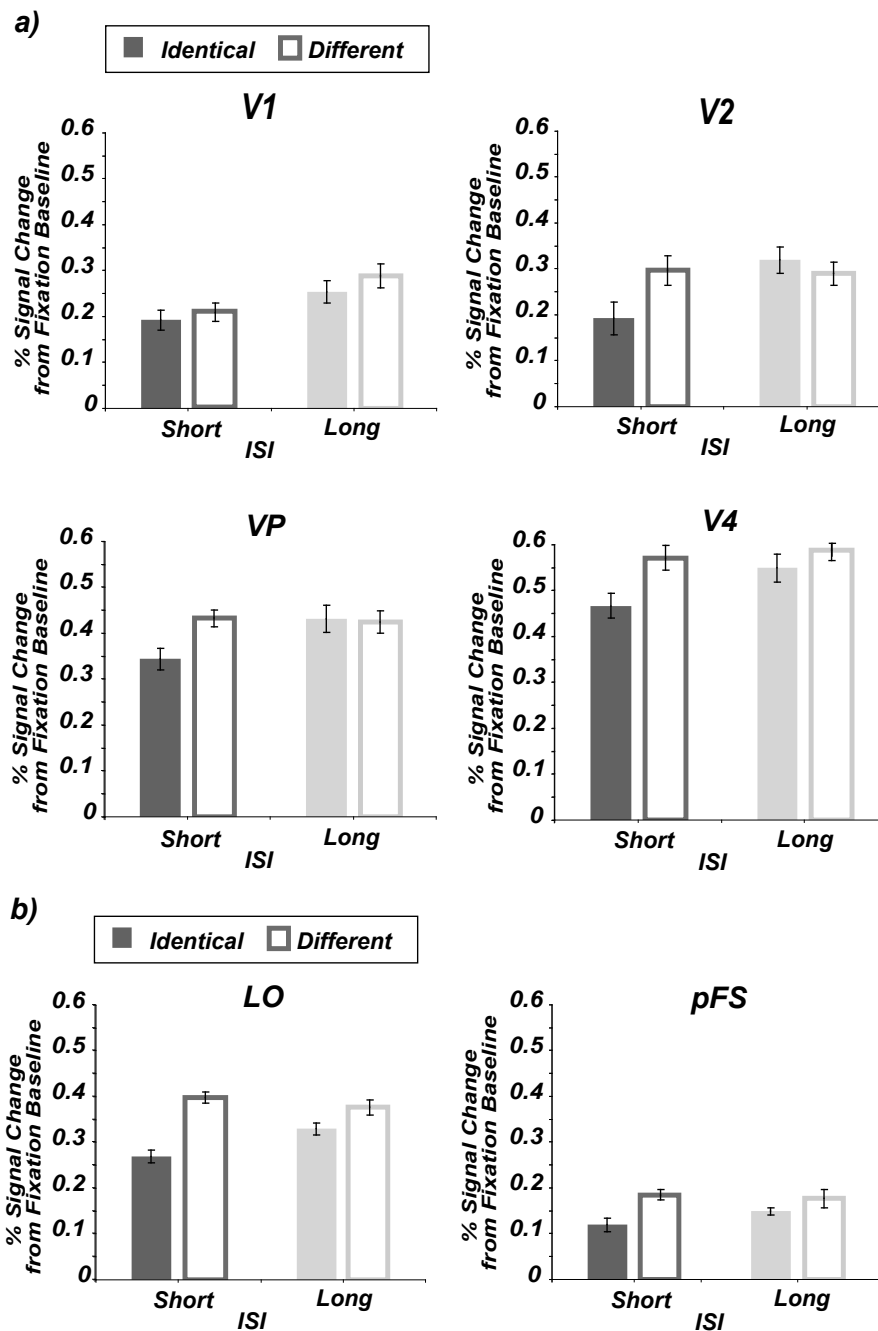


Figure 3.2: fMRI responses for Experiment 2. Displayed are the averaged normalized responses (Percent Signal Change from Fixation Baseline) across measurements (3 to 5 sec after the onset of a trial) and subjects in a) early visual areas (V1, V2, VP and V4); and b) the subdivisions of the LOC (LO and pFs). Error bars indicate the standard error across subjects.

### 3.3 Results for Experiment 3

Experiment 3 tested for the temporal characteristics of shape processing underlying adaptation at high temporal resolution in a MEG study.

Adaptation, that is lower amplitudes for trials with identical compared to different shapes of the LOC FOI, was observed for both ISIs. These differences occurred at latencies corresponding to the presentation of the second stimulus, whereas no differences were observed at earlier latencies. Specifically, t-tests showed significantly lower responses in an interval between 150 and 300 msec after the onset of the second stimulus at the level of  $p < 0.007$  for the short ISI and at the level of  $p < 0.004$  for the long ISI. These findings are consistent with previous fMRI and MEG studies (Malach et al., 1995; Goebel et al., 1998; Hopf et al., 2000) and the present findings of Experiment 1 and 2 and further suggest an involvement of higher occipito-temporal areas in the analysis of shape information.

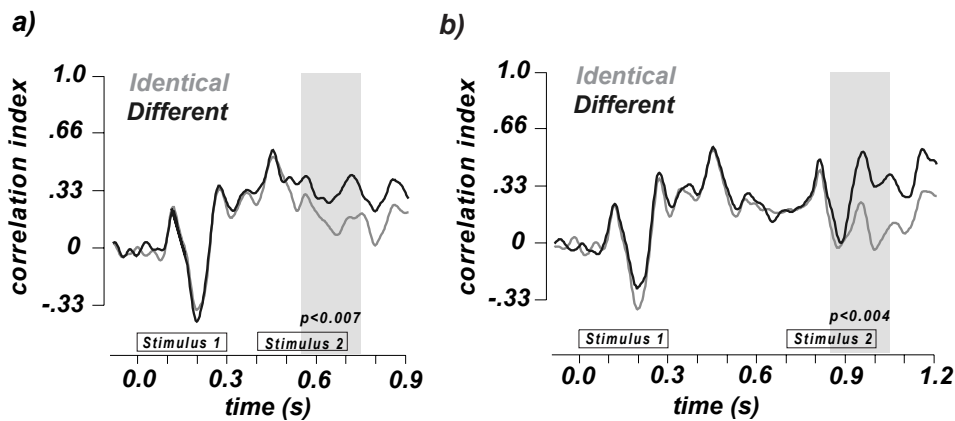


Figure 3.3: Correlation index for Experiment 3. Displayed are the correlation indices between the LOC - Field of Interest and the observed magnetic fields for the a) short ISI and b) long ISI. Significant intervals between consecutively identical and different stimuli were observed at an interval of 150 to 300 msec after the onset of the second stimuli in a trial for both ISIs.

## 3.4 Results for Experiment 4

Experiment 4 tested for adaptation effects at different spatial scales following orientation changes of local Gabor elements without position changes or changes of global shapes.

Strong fMRI adaptation effects to local changes, that is changes in the orientation of the local Gabor elements by 90 degrees, were observed in early visual areas (V1, V2, VP and V4) and to a smaller extent also in the subdivisions of the LOC (LO and pFs). In contrast, fMRI adaptation effects to global changes, that is changes in the global shape, were found in the LO and pFs. However, these adaptation effects did not occur in V1, V2, VP and V4.

Specifically, a repeated measures ANOVA with Global Change (Identical Shape, Different Shape), Local Change (Identical Orientation, Different Orientation), and ROI (V1, V2, VP, V4, LO and pFs) as independent factors showed significant main effects of Local Change ( $F [1, 11] = 5.42, p < 0.05$ ) and ROI ( $F [1, 11] = 8.44, p < 0.001$ ), but not Global Change ( $F [1, 11] < 1, p = 1.0$ ). A significant interaction of ROI and Global Change ( $F [5, 55] = 12.61, p < 0.001$ ) was observed. Contrast analysis showed significant stronger responses for trials of stimuli with different than identical orientations of local Gabor elements in V1 ( $F [5, 55] = 11.10, p = 0.001$ ), V2 ( $F [5, 55] = 48.61, p < 0.001$ ), VP ( $F [5, 55] = 18.44, p < 0.001$ ), V4 ( $F [5, 55] = 16.02, p < 0.001$ ) and LO ( $F [5, 55] = 5.40, p < 0.05$ ), but only a trend in pFs ( $F [5, 55] = 2.95, p = 0.09$ ). Furthermore, significant stronger responses for different than identical global shapes were found in LO ( $F [5, 55] = 19.94, p < 0.001$ ) and pFs ( $F [5, 55] = 10.34, p < 0.01$ ), but not in VP ( $F [5, 55] < 1, p = 0.52$ ) and V4 ( $F [5, 55] < 1, p = 0.76$ ). Interestingly, the opposite pattern was found in V1 ( $F [5, 55] = 5.33, p = 0.02$ ) and V2 ( $F [5, 55] = 24.33, p < 0.001$ ) resulting from stronger fMRI responses for changes in the orientation of local Gabor elements than changes in the global shape.

In summary, these results indicate neural sensitivity to local orientation changes primarily for early visual areas. In contrast, the LOC showed sensitivity to changes of the global shape. Consistent with recent studies (Smith et al., 2002;

Kourtzi et al., 2003b), these findings suggest an involvement of early visual areas in local contour integration processes and higher visual areas at global scales. Finally, the findings suggest a possible influence of global shape processing in higher visual areas on the processing of local features at the early stages of cortical processing consistent with previous reports (Rao & Ballard, 1999; Murray et al., 2002, 2004).



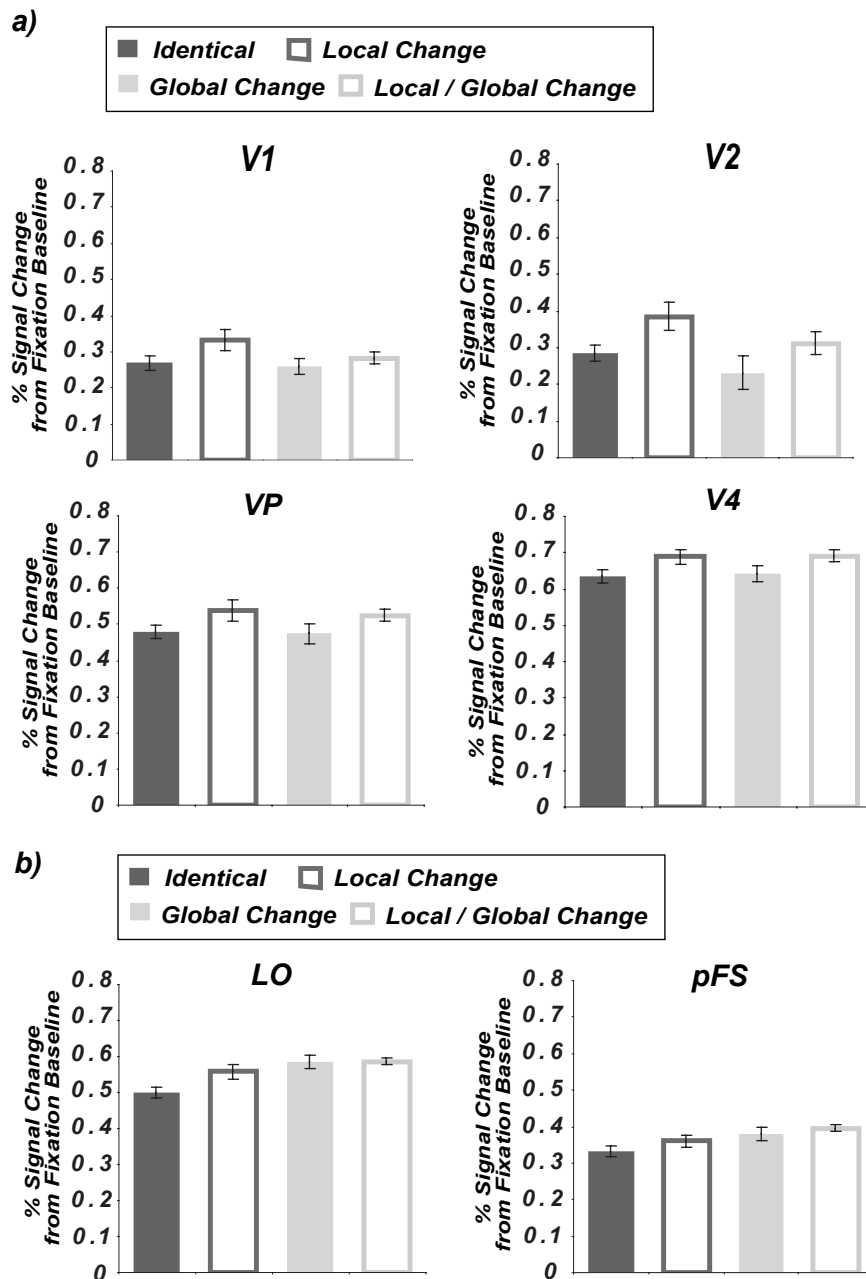


Figure 3.4: fMRI responses for Experiment 4. Displayed are the averaged normalized responses (Percent Signal Change from Fixation Baseline) across measurements (3 to 5 sec after the onset of a trial) and subjects in a) early visual areas (V1, V2, VP and V4); and b) the subdivisions of the LOC (LO and pFs). Error bars indicate the standard error across subjects.

### 3.5 Results for Experiment 5

Experiment 5 tested for adaptation effects to changes in the orientation of a random field of Gabor elements. fMRI adaptation effects were observed to changes in the orientation of local Gabor elements in the early visual areas (V1, V2, VP and V4), but not the subdivisions of the LOC (LO and pFs). Furthermore, fMRI responses to repeated presentations were higher than to single presentations in early and higher visual areas (V1, V2, VP, V4, LO and pFs) and showed the highest degree of linear summation of fMRI responses to repeated presentations compared to single presentations in the subdivisions of the LOC.

Specifically, a repeated measures ANOVA with Condition (Single Presentation, Repeated Presentation / Identical Orientation, Repeated Presentation / Different Orientation) and ROI (V1, V2, VP, V4, LO and pFs) as independent factors showed significant main effects of Condition ( $F [2, 18] = 57.11, p < 0.001$ ) and ROI ( $F [5, 45] > 1000, p < 0.001$ ). A significant interaction of ROI and Condition ( $F [10, 90] = 7.21, p < 0.001$ ) was observed. Contrast analysis showed significantly stronger responses for different than identical orientations of Gabor elements in V1 ( $F [10, 90] = 10.11, p < 0.01$ ), V2 ( $F [10, 90] = 5.30, p < 0.05$ ), VP ( $F [10, 90] = 12.02, p < 0.001$ ), V4 ( $F [10, 90] = 5.30, p < 0.05$ ) and a trend in LO ( $F [10, 90] = 3.71, p = 0.06$ ), but no difference in pFs ( $F [10, 90] < 1, p = 0.56$ ). Further contrast analysis showed significantly stronger responses for Repeated Presentation / Identical Orientation compared to Single Presentation for all ROIs (V1:  $F [10, 90] = 92.63, p < 0.001$ , V2:  $F [10, 90] = 73.05, p < 0.001$ , VP:  $F [10, 90] = 63.79, p < 0.001$ , V4:  $F [10, 90] = 105.11, p < 0.001$ , LO:  $F [10, 90] = 10.92, p < 0.01$  and pFs:  $F [10, 90] = 20.49, p < 0.001$ ).

In summary, these results confirmed the findings of Experiment 4 indicating a decrease of neural selectivity in the processing of local features from early to higher visual areas. Additionally, a high degree of linear summation of fMRI responses were observed in higher and to a lower degree in early visual areas.

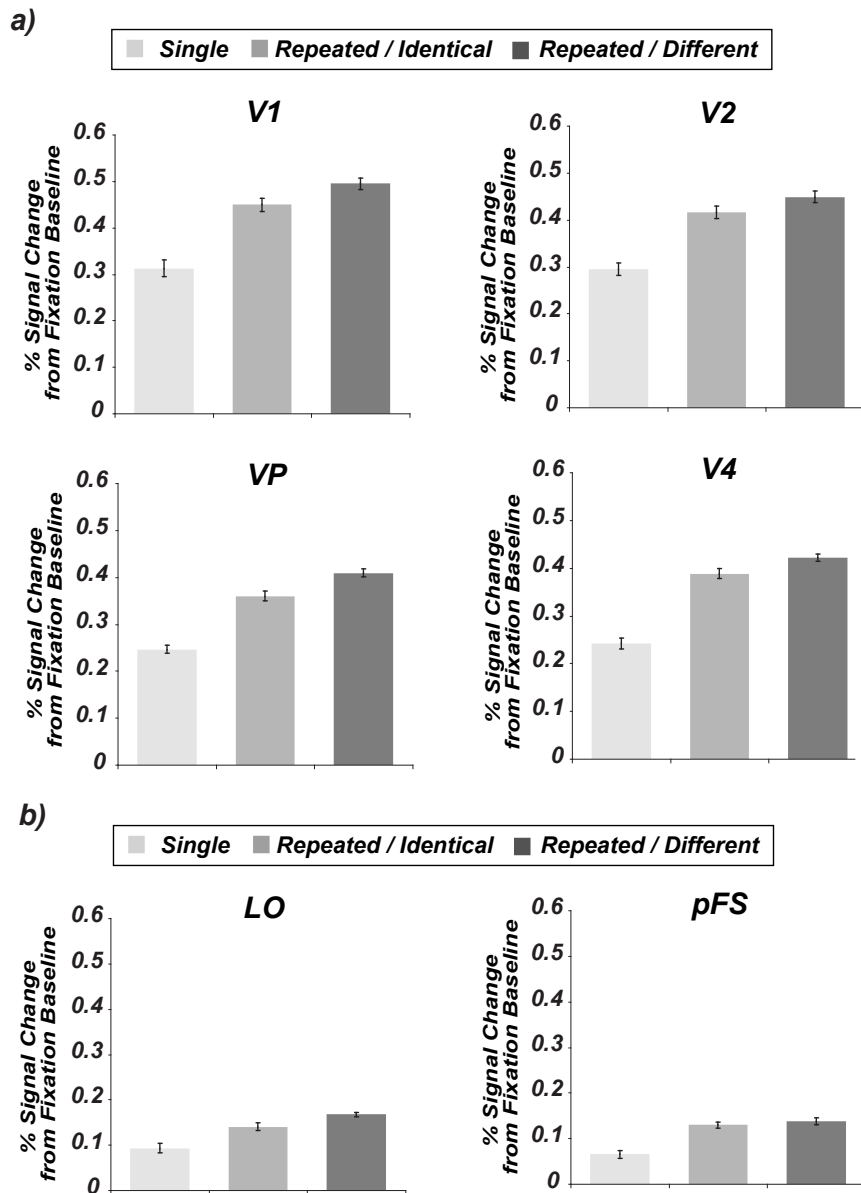


Figure 3.5: fMRI responses for Experiment 5. Displayed are the averaged normalized responses (Percent Signal Change from Fixation Baseline) across measurements (3 to 5 sec after the onset of a trial) and subjects in a) early visual areas (V1, V2, VP and V4); and b) the subdivisions of the LOC (LO and pFs). Error bars indicate the standard error across subjects.



# Chapter 4

## Discussion

Based on the results of recent studies, that suggested an involvement of early and higher visual areas in the processing of shape information (Smith et al., 2002; Kourtzi et al., 2003b), our studies aimed at investigating the spatiotemporal characteristics of early and higher visual areas in the analysis of shape information at different temporal (variation in the stimulus presentation rates) and spatial (global shape vs. local features) scales in combined fMRI and MEG studies.

### **4.1 What is the advantage of combined fMRI and MEG studies ?**

Over the past decade, fMRI has become a sensitive tool to investigate the functional properties of the primate brain. At the current stage of investigation, many questions about the nature of the BOLD signal remain open. However, recent studies (Logothetis et al., 2001) provide strong evidence for a close correlation between the BOLD signal and local field potentials, which are believed to reflect the spiking activity of neurons (for review see Heeger & Ress, 2002). Therefore, these results further strengthen the role of fMRI as powerful tool for the non-invasive investigation of the human brain at decent spatial resolution. Although fMRI cannot reach the unique spatial resolution of single cell recordings, fMRI adaptation paradigms (Buckner et al., 1998; Grill-Spector et al., 1999; Kourtzi et

al., 2003a) have been established to overcome the limited spatial resolution of fMRI and allow the investigation of the functional properties of small numbers of neurons. The major limitation of fMRI is found in its poor temporal resolution in the range of seconds. In contrast, MEG provides excellent temporal resolution at medial spatial resolution. Thus, the combination of both techniques, facilitates the non-invasive investigation of the human brain at high spatial and temporal resolution.

## **4.2 What are the temporal characteristics of shape processing across early and higher visual areas ?**

The present findings indicate a transient processing of shape information in early visual areas compared to a rather sustained analysis in higher visual areas along the ventral visual pathway (Experiment 1). These findings are consistent with previous imaging studies in the human brain, that showed prolonged activation for the presentation of objects in occipito-temporal areas compared to early visual areas or motion processing (hMT+/V5) areas (Ferber et al., 2003; Henson et al., 2004; Mukamel et al., 2004) and are in accordance with recent electrophysiological studies testing the role of neurons in the inferotemporal cortex of the macaque (Miyashita & Chang, 1988; Desimone, 1996; Brown & Xiang, 1998; Tamura & Tanaka, 2001). Finally the results are in agreement with previous studies, that investigated the role of rapid adaptation in complex cells of primary visual cortex in the macaque (Müller et al., 1999). These studies showed enhanced neuronal selectivity at an ISI below 200 msec, while adaptation was not observed at an extended ISI.

However, sustained processing of shape information may also mediate visual short-term memory for objects (Potter, 1976; Intraub, 1980) and facilitate learning mechanisms (Yakovlev et al., 1998). It could be argued, that the observers paid more attention to conditions with a change of the global shape than in trials with

consecutively identical stimuli. Analysis of the behavioral responses of the observers indicated a performance close to the maximum of 100 %, but showed in agreement with previous studies faster reaction times for identical than different shapes in a trial. Experiment 2 further controlled for the possibility of attentional confounds by introducing a dimming task (detection of luminance changes) on the fixation point to the paradigm of Experiment 1. This task required similar attentional mechanisms across conditions and thus entailed a comparable attentional load. The findings of Experiment 2 replicated the results observed in Experiment 1 and thus argues against an extended role of attention in the temporal characteristics of early and higher visual areas.

At what latencies do adaptational mechanisms in the processing of shape information appear in higher visual areas of the ventral visual pathway?

In accordance to earlier "Sensor of Interest" analysis (Liu et al., 2000, 2002, Downing et al., 2001), the present work introduced a "Field of Interest" analysis for the LOC. The close relation between the locations of the dipoles for the LOC and the independently defined voxels in the fMRI study as well as the high percentage of variance that could be explained by these dipoles further support the validity of the LOC FOI. In comparison to the FOI analysis, the SOI approach enables the investigation of individual sensors, whereas the FOI analysis includes magnetic field and rather accounts for a spatially distributed area. Second, in addition to the ROI analyses conducted in fMRI, the FOI approach provides an excellent temporal resolution.

Adaptation was observed for the short and the long ISI for the LOC at a temporal interval of 150 to 300 msec after the onset of the second stimulus. These findings are consistent with previous findings (Hopf et al., 2000), that reported similar effects at latencies of 220 to 240 msec at occipitotemporal sources and are also in agreement with the findings of Experiment 1 and 2. Thus, the present findings suggest differential processing for the presentation of consecutively identical compared to different shapes in a trial not only using imaging techniques but also non-invasive electrophysiological methods like MEG and further strengthen the role of fMRI adaptation paradigms as a sensitive tool to investigate the func-

tional properties of the primate brain and overcome the limited spatial resolution of conventional fMRI.

### **4.3 What are the spatial characteristics of shape processing across early and higher visual areas ?**

Experiment 4 indicated reduced neural sensitivity to changes in the orientation of local Gabor elements increasing along a hierarchy of visual areas that extends from primary visual cortex to higher areas in the posterior fusiform gyrus and are consistent with previous studies investigating the orientation selectivity of early visual areas (Carandini et al., 1997). In contrast, sensitivity to changes in the global shape suggested a reversed pattern. That is, global selectivity increased from early to higher visual areas.

Do these results contradict the adaptation effects observed in Experiment 1? The mean overlap of global shapes used in Experiment 1 was 72.20 % suggesting that the rebound of the fMRI responses during the presentation of different shapes likely underlied changes in the global shapes by small changes in the orientation of the local Gabor elements rather than the changes in the position of the global shapes and therefore the involvement of different receptive fields. Thus, these findings for the early visual areas are in agreement with previous work suggesting an involvement of early visual areas in the analysis of global shape information by integration mechanisms, that exceeded the size of classical receptive fields and were linked to the processing of the orientation of the local contour (Sceniak et al., 1999; Smith et al., 2002; Kourtzi et al., 2003a). In contrast to early visual areas, higher visual areas appear to represent the perceived global shape (Kourtzi & Kanwisher, 2001) as well as salient shape regions (Stanley & Rubin, 2003). Further, they have been shown to represent the global shape invariant of local image changes (Grill-Spector et al., 1999). Thus, these areas may encode shape information independent of the organization of their local elements. What mech-



anisms might enable shape processing in early visual areas in a rather global fashion? The role of feedback connections from higher to early visual areas have been investigated in a number of studies (Edelman, 1992; Nowak & Bullier, 1998; Roelfsema et al., 1998). These recurrent connections may modulate the integration of local features together with the horizontal connections within primary visual cortex, that have been proposed to link neurons of similar orientation tuning and mediate contour integration (Gilbert, 1992, 1998) and enable the processing of shape information in a global fashion in early visual areas (Lamme et al., 1998; Lamme & Roelfsema, 2000; Bullier, 2001). However, the interpretation of the different effects in higher visual areas across the current experiments might also propose a role of the type of stimulus.

In Experiment 1 and 2, global shapes were tested consisting of local Gabor elements that were aligned along the contour, while these elements had the same orientation in Experiment 4 and were thus parallel to each other, but not aligned along the contour. Where do these grouping patterns occur in nature? The alignment of oriented elements along the contour of a shape appears frequently in many natural images and has been shown together with good continuation to play a role in the processing of visual information in primary visual cortex (Koffka, 1935; Sigman et al., 2001, Kapadia et al., 1995). Further, these shapes induce a pop-out effect in cluttered scenes resulting in easy detection (Field et al., 1993; Hess et al., 2003). Moreover, modulation of V1 activity has been suggested to be strongly influenced by the perceptual level of shapes that is facilitated by pop-out effects (Super et al., 2001). In contrast, shapes consisting of elements that are organized parallel to each other and show the same orientation are rather applied in textured surfaces than natural images (Geisler et al., 2001; Hess et al., 2003). In addition, these shapes have been suggested to inhibit responses in the primary visual cortex (Born & Tootell, 1991). Thus, our findings may indicate differential neuronal mechanisms underlying the processing of our stimuli.

## 4.4 What is the role of attention in the processing of shape information?

Previous studies (Murray & Wojciulik, 2004) suggested a role of attention in the processing of shape information in higher visual areas with enhanced BOLD activity for attended compared to non-attended objects in the LOC. In parallel, similar findings were also observed in V1 (Gilbert et al., 2000). In summary, attention is required for the processing of shape information in primary visual cortex and occipito-temporal areas (Roelfsema et al., 1998). The present results of Experiment 1 and 2 are in agreement with these findings and indicate a critical role of attentional modulation in the spatiotemporal properties of integration mechanisms in the human visual cortex. Additionally, the results suggest, that global attention enhances the sustained processing of global shape information. In contrast, the enhanced responses for attended (Experiment 1) compared to non-attended (Experiment 2) shapes in primary visual cortex cannot simply be explained by feedforward connections from the lateral geniculate nucleus via V1 to subsequent processing in occipito-temporal areas but rather indicate a role of feedback connections from higher to early visual areas as well as horizontal connections within V1. These connections not only enhance but also prolong the neuronal representations of attended stimuli in primary visual cortex (Schroeder et al., 2001). Thus, activity of neurons in primary visual cortex likely remains enhanced after the participation in a feedforward sweep (Edelman, 1992; Lamme & Roelfsema, 2000) and is modulated at later steps, that reach a perceptual level, by feedback connections. This observation might be explained by ideas suggesting that adaptation may also reflect changes in the prediction error (Friston, 2002). According to this model, a preliminary prediction is made at the initial processing of shape information in primary visual cortex. The prediction error is then reduced via feedback connections from higher visual areas.

In addition, it has been shown, that divided attention facilitates the integration of collinearly oriented local features (Ito et al., 1998; Ito & Gilbert, 1999; Roberts et al., 2005). Interestingly, the present results not only suggest a role of local

attention in the sustained processing of objects defined by collinearly oriented local elements but extend it also for integrations mechanisms of local elements oriented in parallel.

## **4.5 Outlook**

In the past, a number of visual disorders has been investigated using fMRI. These disorders include impairments in object (James et al., 2003) or more specific face (prosopagnosia) recognition (Takahashi et al., 1995). Besides patient oriented investigation, the BOLD signal has been shown to alterate with ageing (for review see: D'Esposito et al., 2003). However, at the current stage of investigation many questions about the spatiotemporal characteristics of shape processing in elderly people and patients with visual disorders remain open.

Further, future studies are required for the investigation of more complex integration processes (i.e. local contours to objects and multiple objects to scenes) that are shown to implicate higher temporal and parietal cortical areas (Fink et al., 1996).



# Chapter 5

## Conclusions

In summary, the present work suggests that event-related fMRI adaptation paradigms are a sensitive tool to investigate shape analysis at different spatial and temporal scales across visual areas in the human brain. In detail, the findings indicate processing of shape information in early visual areas is transient and restricted to a local neighborhood around the receptive fields of their cells resulting in an analysis at high spatiotemporal resolution. In contrast, a rather coarse spatiotemporal resolution is implemented in the processing of shape information in higher visual areas resulting in sustained analysis. Further, recurrent processing between early and higher visual areas via feedforward and feedback projections might play a critical role in local-to-global and global-to-local mechanisms in shape analysis following prior knowledge about the organization of natural scenes and demands. Finally, combined fMRI and MEG studies allow the investigation at high temporal and spatial resolution.



# Chapter 6

## Summary

Recent studies have shown that global information about shapes is processed in both early ventral (i.e. V1, V2, Vp, V4) and higher occipitotemporal visual areas (i.e. Lateral Occipital Complex/LOC). However, the temporal and spatial properties of shape processing across visual areas in the human brain are largely unknown.

The present thesis addressed this question in a combined fMRI and MEG study, that made use of the complimentary spatial and temporal resolution of the two techniques. An event-related adaptation paradigm was applied, in which lower neural responses are observed for two identical than two different consecutively-presented stimuli. The stimuli were shapes, that consisted of collinear Gabor elements. To investigate the temporal properties of shape processing, the inter-stimulus interval between the two consecutively-presented stimuli was manipulated (ISI: 100 vs. 400 msec). The results showed adaptation for both the short and the long ISI in the LOC, but only for the short ISI in early visual areas. Further, the spatial properties (Local vs. Global) were tested by changes in the local orientation of the Gabor elements or different global changes. Strong fMRI adaptation effects to local changes were observed in early visual areas (V1, V2, VP and V4) and to a smaller extent also in LOC. In contrast, fMRI adaptation effects to global changes were found only for the LOC, but not the early visual areas.

In summary, the findings indicated, that processing of shape information in early

visual areas is transient and restricted to a local neighbourhood around the receptive fields of their cells resulting in an analysis at high spatiotemporal resolution in early visual areas. In contrast, a rather coarse spatiotemporal resolution is implemented in the processing of shape information in higher visual areas resulting in sustained analysis. Further, recurrent processing between early and higher visual areas via feedforward and feedback projections might play a critical role in local-to-global and global-to-local mechanisms in shape analysis. In addition, the experiments confirmed the role of event-related fMRI adaptation paradigms as a sensitive tool to study shape analysis at different spatial and temporal scales across visual areas in the human brain and finally indicated that combined fMRI and MEG studies allow the investigation at high temporal and spatial resolution.



# Chapter 7

## References

Allman J., Miezin F., McGuinness E., 1985. Stimulus specific responses from beyond the classical receptive field: neurophysiological mechanisms for local - global comparisons in visual neurons. *Annu. Rev. Neurosci.* 8, 407-430.

Altmann C.F., Bühlhoff H.H., Kourtzi Z., 2003. Perceptual organization of local elements into global shapes in the human visual cortex. *Curr. Biol.* 13, 342-349.

Avidan G., Hasson U., Hendler T., Zohary E., Malach R., 2002. Analysis of the neuronal selectivity underlying low fMRI signals. *Curr. Biol.* 12, 964-972.

Born R.T., Tootell R.B., 1991. Single-unit and 2-deoxyglucose studies of side inhibition in macaque striate cortex. *Proc. Natl. Acad. Sci. U. S. A.* 88, 7071-7075.

Boynton G.M., Engel S.A., Glover G.H., Heeger DJ., 1996. Linear systems analysis of functional magnetic resonance imaging in human V1. *J. Neurosci.* 16, 4207-4221.

Brown M.W., Xiang, J.Z., 1998. Recognition memory: neuronal substrates of the judgement of prior occurrence. *Prog. Neurobiol.* 55, 149-189.

Buckner R.L., 1998. Event-related fMRI and the hemodynamic response. *Hum. Brain Mapp.* 6, 373-377.

Buckner R.L., Goodman J., Burock M., Rotte M., Koutstaal W., Schacter D., Rosen B., Dale A.M., 1998. Functional-anatomic correlates of object priming in humans revealed by rapid presentation event-related fMRI. *Neuron* 20, 285-296.

Bullier J., 2001. Integrated model of visual processing. *Brain Res. Brain Res. Rev.* 36, 96-107.

Bullier J., Hupe J.M., James A.C., Girard P., 2001. The role of feedback connections in shaping the responses of visual cortical neurons. *Prog. Brain Res.* 134, 193-204.

Carandini M., Barlow H.B., O'Keefe L.P., Poirson A.B., Movshon J.A., 1997. Adaptation to contingencies in macaque primary visual cortex. *Philos. Trans. R. Soc. Lond., Ser. B Biol. Sci.* 352, 1149-1154.

Churchland P.S., Sejnowski T.J., 1988. *Perspectives on Cognitive Neuroscience*, *Science* 242, 741-745.

Cohen D., 1968. Magnetoencephalography: evidence of magnetic fields produced by alpha-rhythm currents. *Science* 161, 784-6.

Cohen M.S., 1997. Parametric analysis of fMRI data using linear systems methods. *Neuroimage* 6, 93-103.

Denys K., Vanduffel W., Fize D., Nelissen K., Peuskens H., Van Essen D., Orban G.A., 2004. The processing of visual shape in the cerebral cortex of human and nonhuman primates: a functional magnetic resonance imaging study. *J. Neurosci.* 24, 2551-65.

Desimone R., 1996. Neural mechanisms for visual memory and their role in attention. *Proc. Natl. Acad. Sci. U S A* 93, 13494-9.

D'Esposito M., Deouell L.Y., Gazzaley A., 2003. Alterations in the BOLD fMRI signal with ageing and disease: a challenge for neuroimaging. *Nat. Rev. Neurosci.* 4, 863-72.

DeYoe E.A., Carman G.J., Bandettini P., Glickman S., Wieser J., Cox R., Miller D., Neitz J., 1996. Mapping striate and extrastriate visual areas in human cerebral cortex. *Proc. Natl. Acad. Sci. U S A* 93, 2382-2386.

DeYoe E.A., Van Essen D.C., 1988. Concurrent processing streams in monkey visual cortex. *Trends Neurosci.* 11, 219-26.

Downing P., Liu J., Kanwisher N., 2001. Testing cognitive models of visual attention with fMRI and MEG. *Neuropsychologia* 39, 1329-1342.

Eger E., Henson R.N., Driver J., Dolan R.J., 2004. BOLD repetition decreases in object-responsive ventral visual areas depend on spatial attention. *J. Neurophysiol.* 92, 1241-1247.

Engel S.A., Furmanski C.S., 2001. Selective adaptation to color contrast in human primary visual cortex. *J. Neurosci.* 21, 3949-3954.

Engel S.A., Rumelhart D.E., Wandell B.A., Lee A.T., Glover G.H., Chichilnisky E.J., Shadlen M.N., 1994. fMRI of human visual cortex. *Nature* 369, 525.

Edelman S., 1992. Visual Perception, in the *Encyclopedia of Artificial Intelligence* 2, 1655-1663.

Essen D.C., Zeki S.M., 1978. The topographic organization of rhesus monkey prestriate cortex. *J. Physiol.* 277, 193-226.

Felleman D.J., Van Essen D.C., 1991. Distributed hierarchical processing in the primate cerebral cortex. *Cereb. Cortex* 1, 1-47.

Ferber S., Humphrey G.K., Vilis T., 2003. The lateral occipital complex subserves the perceptual persistence of motion-defined groupings. *Cereb. Cortex* 13, 716-721.

Field D.J., Hayes A., Hess R.F., 1993. Contour integration by the human visual system: evidence for a local 'association field'. *Vision Res.* 33, 173-193.

Fink G.R., Halligan P.W., Marshall J.C., Frith C.D., Frackowiak R.S., Dolan R.J., 1996. Where in the brain does visual attention select the forest and the trees? *Nature* 382, 626-628.

Foster K.H., Gaska J.P., Nagler M., Pollen D.A., 1985. Spatial and temporal frequency selectivity of neurons in visual cortical areas V1 and V2 of the macaque monkey. *J. Physiol.* 365, 331-63.

Friston K., 2002. Functional integration and inference in the brain. Review. *Prog. Neurobiol.* 68, 113-43.

Fukushima K., 1980. Neocognition: a self-organizing neural network model for a mechanism of pattern recognition unaffected by shift in position. *Biological Cybernetics*, 36, 193-202.

Geisler W.S., Perry, J.S., Super, B.J., Gallogly, D.P., 2001. Edge cooccurrence in natural images predicts contour grouping performance. *Vision Res.* 41, 711-724.

Gilbert C.D., 1992. Horizontal integration and cortical dynamics. *Neuron* 9, 1-13.

Gilbert C.D., 1998. Adult cortical dynamics. *Physiol. Rev.* 78, 467-485.

Gilbert C., Ito M., Kapadia M., Westheimer G., 2000. Interactions between attention, context and learning in primary visual cortex. *Vision Res.* 40, 1217-1226.

Goebel R., Khorrám-Sefat D., Muckli L., Hacker H., Singer W., 1998. The constructive nature of vision: direct evidence from functional magnetic resonance imaging studies of apparent motion and motion imagery, *Eur. J. Neurosci.* 10, 1563-1573.

Grill-Spector K., 2003. The neural basis of object perception. *Curr. Opin. Neurobiol.* 13, 159-166.

Grill-Spector K., Malach R., 2001. fMR-adaptation: a tool for studying the functional properties of human cortical neurons. *Acta Psychol. (Amst.)* 107, 293-321.

Grill-Spector K., Kushnir T., Hendler T., Malach R., 2000. The dynamics of object-selective activation correlate with recognition performance in humans. *Nat. Neurosci.* 3, 837-843.

Grill-Spector K., Kushnir T., Edelman S., Itzhak Y., Malach R., 1998a. Cue-invariant activation in object-related areas of the human occipital lobe. *Neuron* 21, 191-202.

Grill-Spector K., Kushnir T., Hendler T., Edelman S., Itzhak Y., Malach R., 1998b. A sequence of object-processing stages revealed by fMRI in the human occipital lobe. *Hum. Brain Mapp.* 6, 316-328.

Grill-Spector K., Kushnir T., Edelman S., Avidan G., Itzhak Y., Malach R., 1999. Differential processing of objects under various viewing conditions in the human lateral occipital complex. *Neuron* 24, 187-203.

Heeger D.J., Ress D., 2002. What does fMRI tell us about neuronal activity? *Nat Rev. Neurosci.* 3, 142-151.

Henson R.N., Rugg M.D., 2003. Neural response suppression, haemodynamic repetition effects, and behavioural priming. *Neuropsychologia* 41, 263-270.

Henson R.N., Rylands A., Ross E., Vuilleumier P., Rugg M.D., 2004. The effect of repetition lag on electrophysiological and haemodynamic correlates of visual object priming. *Neuroimage* 21, 1674-1689.

Hess R.F., Hayes A., Field D.J., 2003. Contour integration and cortical processing. *J. Physiol. (Paris)* 97, 105-119.

Hopf J.M., Vogel E., Woodman G., Heinze H.J., Luck S.J., 2002. Localizing visual discrimination processes in time and space. *J. Neurophysiol.* 88, 2088-2095.

Huk A.C., Ress D., Heeger D.J., 2001. Neuronal basis of the motion aftereffect reconsidered. *Neuron* 32, 161-172.

Huettel S.A., McCarthy G., 2001. Regional differences in the refractory period of the hemodynamic response: an event-related fMRI study. *Neuroimage* 14, 967-976.

Huettel S.A., Obembe O.O., Song A.W., Woldorff M.G., 2004. The BOLD fMRI refractory effect is specific to stimulus attributes: evidence from a visual motion paradigm. *Neuroimage* 23, 402-408.

Intraub H., 1980. Presentation rate and the representation of briefly glimpsed pictures in memory. *J. Exp. Psychol., Hum. Learn.* 6, 1-12.

Ito M., Gilbert C.D., 1999. Attention modulates contextual influences in the primary visual cortex of alert monkeys. *Neuron* 22, 593-604.

Ito M., Westheimer G., Gilbert C.D., 1998. Attention and perceptual learning modulate contextual influences on visual perception. *Neuron* 20, 1191-1197.

James T.W., Culham J., Humphrey G.K., Milner A.D., Goodale M.A., 2003. Ventral occipital lesions impair object recognition but not object-directed grasping: an fMRI study. *Brain* 126, 2463-75.

Johnson J.S., Olshausen B.A., 2003. Timecourse of neural signatures of object recognition. *J. Vis.* 3, 499-512.

Kanwisher N., Chun M.M., McDermott J., Ledden P.J., 1996. Functional imagining of human visual recognition. *Brain Res. Cogn. Brain Res.* 5, 55-67.

Kapadia K., Ito M., Gilbert C., Westheimer G., 1995. Improvement in visual sensitivity by changes in local context: parallel studies in human observers and in V1 of alert monkeys. *Neuron* 15, 843-856.

Kaufman L., Okada Y., Brenner D., Williamson S.J., 1981. On the relation between somatic evoked potentials and fields. *Int. J. Neurosci.* 15, 223-239.

Koffka, K., 1935. *Principles of Gestalt Psychology*. Harcourt, Brace and Co., New York.

Kourtzi Z., Kanwisher N., 2000. Cortical regions involved in perceiving object shape. *J. Neurosci.* 20, 3310- 3318.

Kourtzi Z., Kanwisher N., 2001. Representation of perceived object shape by the human lateral occipital complex. *Science* 293, 1506- 1509.

Kourtzi Z., Erb M., Grodd W., Bühlhoff H.H., 2003a. Representation of the perceived 3-D object shape in the human lateral occipital complex. *Cereb. Cortex* 13, 911- 920.

Kourtzi Z., Tolias A.S., Altmann C.F., Augath M., Logothetis N.K., 2003b. Integration of local features into global shapes: monkey and human fMRI studies. *Neuron* 37, 333- 346.

Kovacs I., 1996. Gestalten of today: early processing of visual contours and surfaces. *Behav. Brain. Res.* 82, 1-11.

Kovacs I., Julesz B., 1993. A closed curve is much more than an incomplete one: effect of closure in figure-ground segmentation. *Proc. Natl. Acad. Sci. U. S. A.* 90, 7495-7497.

Kovacs I., Julesz B., 1994. Perceptual sensitivity maps within globally defined visual shapes. *Nature* 370, 644-646.

Kovacs I., Kozma P., Feher A., Benedek G., 1999. Late maturation of visual spatial integration in humans. *Proc. Natl. Acad. Sci. U S A* 96, 12204-12209.

Kristeva-Feige R., Feige B., Makeig S., Ross B., Elbert T., 1993. Oscillatory brain activity during a motor task. *Neuroreport* 4, 1291-1294.

Kruggel F., von Cramon D.Y., 1999. Modeling the hemodynamic response in single-trial functional MRI experiments. *Magn. Reson. Med.* 42, 787-797.

Lamme V.A., Roelfsema P.R., 2000. The distinct modes of vision offered by feed-forward and recurrent processing. *Trends Neurosci.* 23, 571-579.

Lamme V.A., Super H., Spekreijse H., 1998. Feedforward, horizontal, and feedback processing in the visual cortex. *Curr. Opin. Neurobiol.* 8, 529- 535.

Lerner Y., Hendler T., Ben-Bashat D., Harel M., Malach R., 2001. A hierarchical axis of object processing stages in the human visual cortex. *Cereb. Cortex* 11, 287-297.

Lisberger S.G., Movshon J.A., 1999. Visual motion analysis for pursuit eye movements in area MT of macaque monkeys. *J. Neurosci.* 19, 2224- 2246.

Liu J., Harris A., Kanwisher N., 2002. Stages of processing in face perception: an MEG study. *Nat. Neurosci.* 5, 910-916.

Liu J., Higuchi M., Marantz A., Kanwisher N., 2000. The selectivity of the occipitotemporal M170 for faces. *Neuroreport* 11, 337-341.

Logothetis N.K., Pauls J., Augath M., Trinath T., Oeltermann A., 2001. Neurophysiological investigation of the basis of the fMRI signal. *Nature* 412, 150-157.

Logothetis N., Sheinberg D., 1996. Visual object recognition. *Annu. Rev. Neurosci.* 19, 577- 621.

Malach R., Reppas J.B., Benson R.R., Kwong K.K., Jiang H., Kennedy W.A., Ledden P.J., Brady T.J., Rosen B.R., Tootell R.B., 1995. Object-related activity revealed by functional magnetic resonance imaging in human occipital cortex. *Proc. Natl. Acad. Sci. U. S. A.* 92, 8135- 8139.

Maunsell J.H., Newsome W.T., 1987. Visual processing in monkey extrastriate cortex. *Annu. Rev. Neurosci.* 10, 363-401.

Menon R.S., Kim S.G., 1999. Spatial and temporal limits in cognitive neuroimaging with fMRI. *Trends. Cogn. Sci.* 3, 207-216.

Milner A.D., Goodale M.A., 1995. *The visual brain in action*. Oxford: Oxford University Press.

Miyashita Y., Chang H.S., 1988. Neuronal correlate of pictorial short-term memory in the primate temporal cortex. *Nature* 331, 68- 70.

Müller J.R., Metha A.B., Krauskopf J., Lennie P., 1999. Rapid adaptation in visual cortex to the structure of images. *Science* 285, 1405-1408.

Mukamel R., Harel M., Hendler T., Malach R., 2004. Enhanced temporal nonlinearities in human object-related occipito-temporal cortex. *Cereb. Cortex* 14, 575-585.

Murray S.O., Kersten D., Olshausen B.A., Schrater P., Woods D.L., 2002. Shape perception reduces activity in human primary visual cortex. *Proc. Natl. Acad. Sci. U. S. A.* 99, 15164- 15169.

Murray S.O., Schrater P., Kersten D., 2004. Perceptual grouping and the interactions between visual cortical areas. *Neural Netw.* 17, 695-705.

Murray S.O., Wojciulik E., 2004. Attention increases neural selectivity in the human lateral occipital complex. *Nat. Neurosci.* 7, 70-74.

Naccache L., Dehaene S., 2001. The priming method: imaging unconscious repetition priming reveals an abstract representation of number in the parietal lobes. *Cereb. Cortex* 11, 966- 974.

Noesselt T., Hillyard S.A., Woldorff M.G., Schoenfeld A., Hagner T., Jancke L., Tempelmann C., Hinrichs H., Heinze H.J., 2002. Delayed striate cortical activation during spatial attention. *Neuron* 35, 575-587.

Nowak L.G., Bullier J., 1998. Axons, but not cell bodies, are activated by electrical stimulation in cortical gray matter. II. Evidence from selective inactivation of cell bodies and axon initial segments. *Exp. Brain. Res.* 118, 489-500.

Ogawa S., Lee T.M, Kay A.R., Tank D.W., 1990a. Brain magnetic resonance imaging with contrast dependent on blood oxygenation. *Proc. Natl. Acad. Sci. U S A* 87, 9868-9872.

Ogawa S., Lee T.M., Nayak A.S., Glynn P., 1990b. Oxygenation-sensitive contrast in magnetic resonance image of rodent brain at high magnetic fields. *Magn.*



Reson. Med. 14, 68-78.

Olson I.R., Chun M.M., Allison T., 2001. Contextual guidance of attention: human intracranial event-related potential evidence for feedback modulation in anatomically early temporally late stages of visual processing. *Brain* 124, 1417-1425.

Pantev C., 1995. Evoked and induced gamma-band activity of the human cortex. *Brain Topogr.* 7, 321-330.

Potter M.C., 1976. Short-term conceptual memory for pictures. *J. Exp. Psychol., Hum. Learn.* 2, 509- 522.

Pulvermuller F., Lutzenberger W., Preissl H., Birbaumer N., 1995. Spectral responses in the gamma-band: physiological signs of higher cognitive processes? *Neuroreport* 6, 2059-2064.

Rao R.P., Ballard D.H., 1999. Predictive coding in the visual cortex: a functional interpretation of some extra-classical receptive-field effects. *Nat. Neurosci.* 2, 79-87.

Raymond J.E., O'Donnell H.L., Tipper S.P., 1998. Priming reveals attentional modulation of human motion sensitivity. *Vision Res.* 38, 2863-2867.

Rezec A., Krekelberg B., Dobkins K.R., 2004. Attention enhances adaptability: evidence from motion adaptation experiments. *Vision Res.* 44, 3035- 3044.

Riesenhuber M., Poggio T., 1999. Hierarchical models of object recognition in cortex. *Nat. Neurosci.* 2, 1019-1025.

Riesenhuber M., Poggio T., 2000. Models of object recognition. *Nat. Neurosci.* 3, 1199- 1204.

Roberts M.J., Zinke W., Guo K., Robertson R., McDonald J.S., Thiele A., 2005. Acetylcholine dynamically controls spatial integration in marmoset primary visual cortex. *J. Neurophysiol.* 93, 2062- 2072.

Roelfsema P.R., Lamme V.A., Spekreijse H., 1998. Object-based attention in the primary visual cortex of the macaque monkey. *Nature* 395, 376-381.

Sceniak M.P., Ringach D.L., Hawken M.J., Shapley R., 1999. Contrast's effect on spatial summation by macaque V1 neurons. *Nat. Neurosci.* 2, 733- 739.

Schroeder C.E., Mehta A.D., Foxe J.J., 2001. Determinants and mechanisms of attentional modulation of neural processing. *Front. Biosci.* 6, 672-684.

Schweitzer L.R., 1991. Binary-choice decision time depends upon cerebral hemisphere and nature of task. *Percept. Mot. Skills* 73, 147-61.

Sereno M.I., Dale A.M., Reppas J.B., Kwong K.K., Belliveau J.W. y Brady T.J., Rosen B.R., Tootell R.B., 1995. Borders of multiple visual areas in humans revealed by functional magnetic resonance imaging. *Science* 268, 889- 893.

Sigman M., Cecchi G.A., Gilbert C.D., Magnasco M.O., 2001. On a common circle: natural scenes and Gestalt rules. *Proc. Natl. Acad. Sci. U. S. A.* 98, 1935-1940.

Smith M.A., Bair W., Movshon J.A., 2002. Signals in macaque striate cortical neurons that support the perception of glass patterns. *J. Neurosci.* 22, 8334-8345.

Stanley D.A., Rubin N., 2003. fMRI activation in response to illusory contours and salient regions in the human lateral occipital complex. *Neuron* 37, 323- 331.

Super H., Spekreijse H., Lamme V.A., 2001. Two distinct modes of sensory processing observed in monkey primary visual cortex (V1). *Nat. Neurosci.* 4, 304-310.

Takahashi N., Kawamura M., Hirayama K., Shiota J., Isono O., 1995. Prosopagnosia: a clinical and anatomical study of four patients. *Cortex* 31, 317-29.

Tamura H., Tanaka K., 2001. Visual response properties of cells in the ventral and dorsal parts of the macaque inferotemporal cortex. *Cereb. Cortex* 11, 384-399.

Tiao Y.C., Blakemore C., 1978. Functional organization of the visual cortex of the golden hamster. *J. Comp. Neurol.* 168, 459-81.

Tootell R.B., Reppas J.B., Dale A.M., Look R.B., Sereno, M.I., Malach R., Brady T.J., Rosen B.R., 1995. Visual motion aftereffect in human cortical area MT revealed by functional magnetic resonance imaging. *Nature* 375, 139- 141.

Tootell R.B., Switkes E., Silverman M.S., Hamilton S.L., 1988. Functional

anatomy of macaque striate cortex. II. Retinotopic organization. *J. Neurosci.* 8, 1531-68.

Ungerleider L.G., Mishkin M., 1982. Two cortical visual systems. In Ingle, D. J., Goodale, M. A., and Mansfield, R. J. W., editors, *Analysis of visual behavior*. The MIT Press, Cambridge, MA.

Van Essen D.C., Anderson C.H., Felleman D.J., 1992. Information processing in the primate visual system: an integrated systems perspective. *Science* 255, 419-423.

VanRullen R., Thorpe S.J., 2001. The time course of visual processing: from early perception to decision-making. *J. Cogn. Neurosci.* 13, 454-461.

Vuilleumier P., Henson R.N., Driver J., Dolan R.J., 2002. Multiple levels of visual object constancy revealed by event-related fMRI of repetition priming. *Nat. Neurosci.* 5, 491- 499.

Wiggs C.L., Martin A., 1998. Properties and mechanisms of perceptual priming. *Curr. Opin. Neurobiol.* 8, 227-233.

Yakovlev V., Fusi S., Berman E., Zohary E., 1998. Inter-trial neuronal activity in inferior temporal cortex: a putative vehicle to generate longterm visual associations. *Nat. Neurosci.* 1, 310- 317.



# Chapter 8

## Appendix

### 8.1 Abbreviations

ANOVA	analysis of variance
BOLD	blood oxygenation level dependent
CBF	cerebral blood flow
CBV	cerebral blood volume
CoS	collateral sulcus
EEG	electroencephalography
fMRI	functional magnetic resonance imaging
FOI	field of interest
GFP	global field power
HRF	hemodynamic response function
ISI	interstimulus interval
IST	inferior temporal sulcus
LGN	lateral geniculate nucleus
LO	lateral occipital
LOC	lateral occipital complex
MEG	magnetoencephalography
MRI	magnetic resonance imaging
OTS	occipital temporal sulcus

PET	positron emission tomography
pFs	posterior fusiform
RF	radiofrequency
ROI	region of interest
SP	stimulus presentation
SQUID	super conducting quantum interference device
STS	superior temporal sulcus
TE	time to echo
TR	time to repetition
2AFC	two alternative forced choice

## 8.2 Supplementary figures

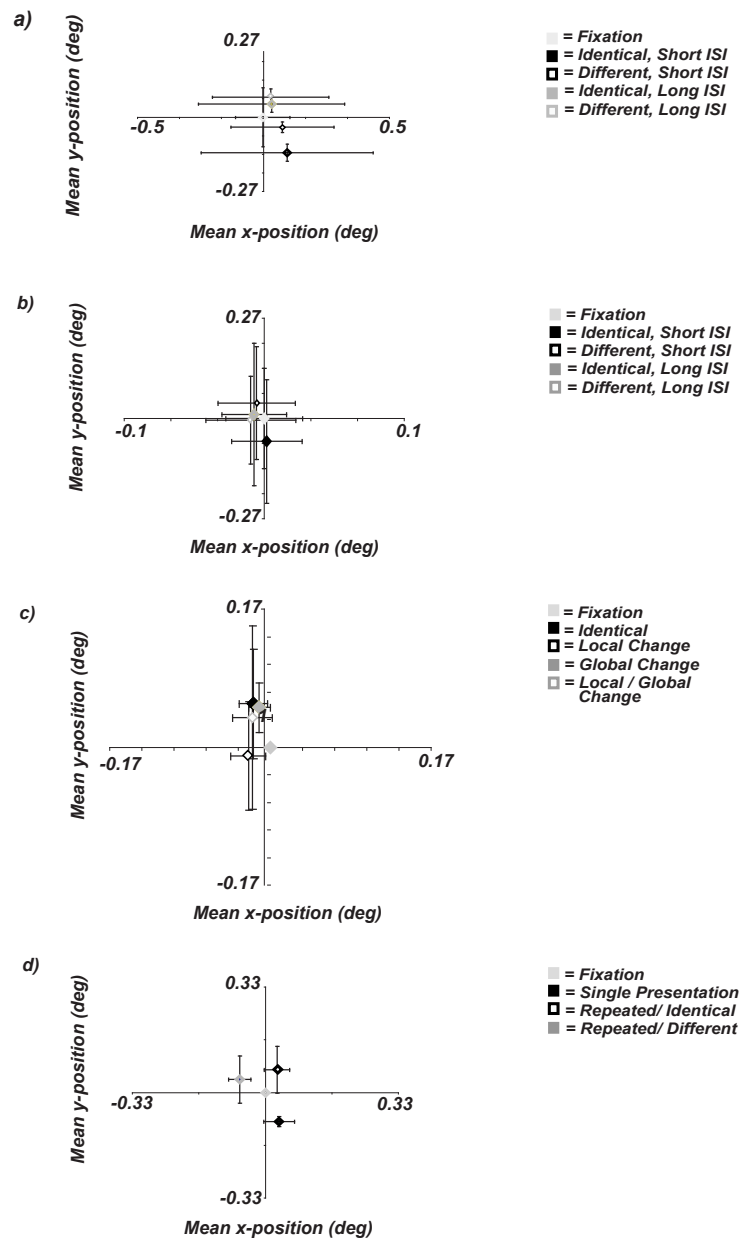


Figure 8.1: Supplementary 1: Mean fixation position for Experiment a) 1 (n=3), b) 2 (n=3), c) 4 (n=4), and d) 5 (n=3). The mean fixation position was similar across conditions.

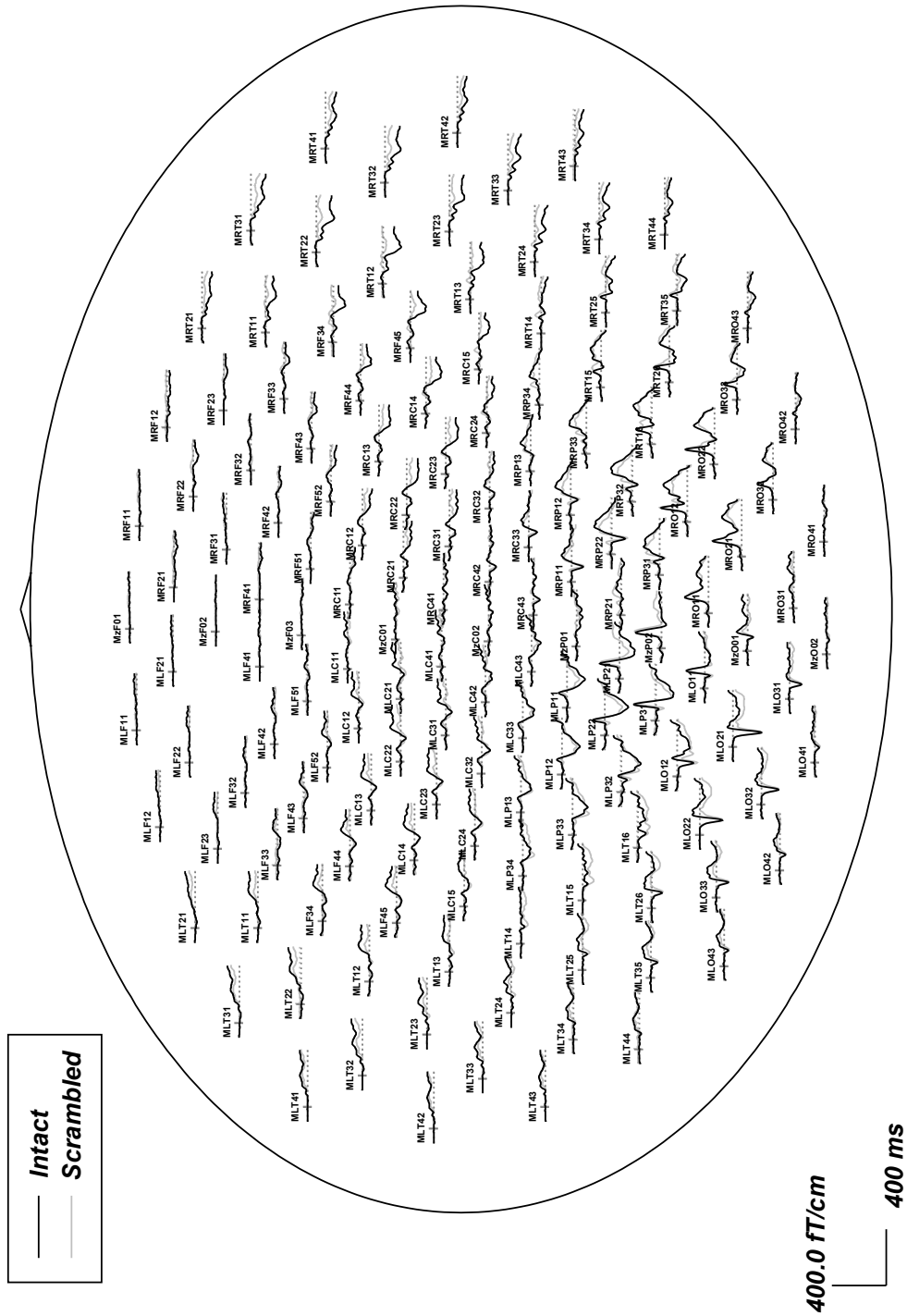


Figure 8.2: Supplementary 2: MEG responses for the LOC localizer averaged across subjects and projected on a flattened head model.



# Chapter 9

## Acknowledgements

Numerous people contributed to the origin of this work and hereby I would like to express my gratefulness to these individuals. First of all, I would like to thank Professor Dr. Zoe Kourtzi and Professor Dr. Dr. Hans-Otto Karnath for their supervision as well as Professor Dr. Heinrich H. Bülthoff and the Max-Planck Society for their support. Furthermore I would like to thank Professor Dr. Wolfgang Grodd and Professor Dr. Werner Lutzenberger for the good collaboration during data collection and analysis. Dr. Michael Erb, Fotini Scherer, Franziska Hösl were always helpful with data collection and technical assistance. I also would like to thank Daniel Berger, Lisa R. Betts, Arne Deubelius, Gerald Franz, Jan Jastorff, Pegah Sarkheil and all the other people at the Max Planck Institute for Biological Cybernetics that contributed to the success of this work. Finally, I would like to thank my family for their unrestricted personal support.



# Chapter 10

## Curriculum vitae

Full name: Elisabeth Huberle  
Date of birth: 01/08/1979  
Place of birth: Berlin

### ***Education***

08/1986 - 07/1990      Grundschule Oberbrüden/Unterbrüden  
08/1990 - 07/1999      Bildungszentrum Weissacher Tal  
10/1999 - 03/2000      Fakultät für Mathematik, Universität Stuttgart  
04/2000 - 11/2006      Fakultät für Medizin, Universität Tübingen

### ***Research experience***

09/2001 - 11/2002      Research assistant at the Max-Planck Institut für Entwicklungsbiologie, Tübingen (Head: Prof. Dr. Bonhoeffer). Topic: retinotectale projection im zebrafish.

09/2002 - 06/2004      Doctoral thesis at the Max-Planck Institut für Biologische Kybernetik, Abteilung für Psychophysik, Tübingen (Head: Prof. Dr. Büllhoff; supervisor: Zoe Kourtzi, PhD) in collaboration with the department Abteilung Kognitive Neurologie, Sektion für Neuropsychologie, Tübingen (Head: Prof. Dr. Dr. Karnath). Topic: Temporal properties of shape processing in the human brain: combined fMRI and MEG studies.

07/2004 - present            Research at the department Kognitive Neurologie, Sektion für Neuropsychologie, Tübingen (Head: Prof. Dr. Dr. Karnath). Topic: Neuronal correlates of feature integration in the human visual cortex.

03/11/2006                    2. Staatsexamen (ÄApO 2002)

### **Conferences**

**Huberle E.**, Lutzenberger W., Bülthoff H.H & Kourtzi Z., 2003. Temporal properties of shape processing across visual areas. Vision Sciences Society, Sarasota, USA.

**Huberle E.**, Kourtzi Z., 2003. Processing of global versus local shape information in the human visual cortex. Society for Neuroscience, New Orleans, USA.

**Huberle E.**, Kourtzi Z., 2004. Global and local mechanisms of shape processing in the human visual cortex. TWK, Tübingen, Germany.

**Huberle E.**, Seymour K., Altmann C.A., Karnath H.-O., 2005. Visual feature integration is a function of the temporo-parieto-occipital junction (TPOJ). Society for Neuroscience, Washington DC, USA.

### **Publications**

Kourtzi Z., **Huberle E.**, 2005. Spatiotemporal characteristics of form analysis in the human visual cortex revealed by rapid event-related fMRI adaptation. *Neuroimage* 28, 440-52.

**Huberle E.**, Karnath H.-O., 2006. Global shape recognition is modulated by the spatial distance of local elements - Evidence from simultanagnosia. *Neuropsychologia* 44, 905-11.